

TECHNICAL UNIVERSITY OF CRETE  
Department of Electronic and Computer Engineering

# Software-Defined Radio Implementation of an OFDM Link

MASTER OF SCIENCE  
IN ELECTRONIC AND COMPUTER ENGINEERING

*Author:*  
Ioannis KARDARAS

*Supervisor:*  
Prof. Athanasios LIAVAS

August 31, 2010

## Acknowledgements

First and foremost, I would like to thank my supervisor, Prof. Athanasios Liavas, for his helpful suggestions and his continuous support. My thanks and appreciation goes to my thesis committee members, Prof. Nikos Sidiropoulos and Prof. George Karystinos. Finally, I would like to extend my heartiest thanks to my friends and members of the telecommunications division.

## **Abstract**

The demand for wireless communications is growing at an explosive pace. Multi-carrier modulation, Orthogonal Frequency Division Multiplexing (OFDM) particularly, has been successfully applied to a wide variety of digital communications applications over the past several years.

OFDM counteracts the intersymbol interference (ISI) introduced by frequency-selective channels and provides high-speed data rate transmissions with low complexity. For this reason, OFDM is widely adopted in many recently standardized broadband communication systems.

Time and frequency synchronization is a crucial issue in an OFDM receiver design. A number of time and frequency synchronization techniques have been proposed. In this thesis, we examine and implement algorithms based on the correlation of two identical parts of an OFDM pilot symbol.

A simple OFDM link has been implemented and tested on a software-defined-radio (SDR) testbed using the Universal Software Radio Peripheral system (USRP). The idea behind SDR is to do all the modulation and demodulation with software instead of using dedicated circuitry. Thus, we can create radios that change on the fly.

# Contents

<b>1</b>	<b>Introduction to OFDM</b>	<b>4</b>
1.1	Multicarrier Modulation . . . . .	4
<b>2</b>	<b>OFDM Structure</b>	<b>6</b>
2.1	OFDM Transmitter . . . . .	6
2.1.1	Signal Representation and Orthogonality . . . . .	6
2.1.2	Cyclic Prefix . . . . .	9
2.2	OFDM Receiver . . . . .	11
<b>3</b>	<b>Channel Estimation</b>	<b>14</b>
<b>4</b>	<b>Synchronization in OFDM systems</b>	<b>17</b>
4.1	Time Synchronization . . . . .	20
4.1.1	Blind Method . . . . .	20
4.1.2	Pilot Based Method . . . . .	27
4.1.3	First and second order statistics of the pilot based metric . . . . .	34
4.1.4	Probability of correct symbol timing synchronization . . . . .	38
4.2	Carrier Frequency Offset Synchronization . . . . .	41
	Appendix 4A: Moments of a zero-mean complex scalar-valued random variable	44
	Appendix 4B: Computation of the mean and variance of the pilot based metric .	45
	Appendix 4C: Variance equality of the real and imaginary part of the pilot based metric . . . . .	51
	Appendix 4D: Asymptotic independence of the pilot based metric for different time indices . . . . .	53
<b>5</b>	<b>Software-Defined Radio using USRP</b>	<b>55</b>
5.1	Software-Defined Radio (SDR) . . . . .	55
5.2	The Universal Software Radio Peripheral System (USRP) . . . . .	56
5.3	Implementation of SDR for OFDM system - Simulations . . . . .	57
	<b>Bibliography</b>	<b>59</b>

# List of Figures

2.1	OFDM Transmitter. . . . .	6
2.2	Orthogonality of the subcarriers. . . . .	9
2.3	Structure of an OFDM block with CP insertion. . . . .	10
2.4	OFDM Receiver. . . . .	11
4.1	Without Frequency Offset, $\epsilon = 0$ . . . . .	19
4.2	Zoom in, one subcarrier. . . . .	19
4.3	With Frequency Offset, $\epsilon \neq 0$ . . . . .	19
4.4	Zoom in. . . . .	19
4.5	Structure of an OFDM synchronization symbol. . . . .	20
4.6	Frequency characteristics of synchronization symbol. . . . .	21
4.7	Structure of an OFDM synchronization symbol. . . . .	24
4.8	Timing Metric - Blind Method, Flat Channel. . . . .	26
4.9	Timing Metric - Blind Method, Frequency Selective Channel. . . . .	27
4.10	Timing Metric - Pilot Based Method. . . . .	32
4.11	Histogram of $d_*$ , 10000 iterations, SNR = 0dB. . . . .	33
4.12	Histogram of $d_*$ , 10000 iterations, SNR = 10dB. . . . .	33
4.13	Variance of $T$ . . . . .	36
4.14	Variance of $T(d_*)$ . . . . .	37
4.15	Probability of correct symbol timing, SNR = 10db. . . . .	40
4.16	Probability of correct symbol timing vs SNR . . . . .	41
5.1	Software radio block diagram. . . . .	56
5.2	The USRP board. . . . .	57
5.3	OFDM diagram. . . . .	57
5.4	Received Signal. . . . .	58
5.5	Real part of the received signal. . . . .	59
5.6	Bit Error Rate. . . . .	60

## Notations

Matrices and vectors are denoted by boldface letters. We use  $E[\cdot]$ ,  $\|\cdot\|$ ,  $(\cdot)$ ,  $(\cdot)^T$  and  $(\cdot)^H$  for expectation, euclidean norm, complex conjugation, transposition and Hermitian transposition, respectively. The notation  $\arg(\cdot)$  indicates the argument of a complex-valued quantity and is defined as  $\arg(x + jy) = \arctan \frac{y}{x}$ . We use  $*$  and  $\otimes$  for linear and cyclic convolution, respectively.

# Chapter 1

## Introduction to OFDM

### 1.1 Multicarrier Modulation

Digital bandpass modulation techniques can be broadly classified into two categories. The first is single-carrier modulation, where data is transmitted by using a single radio frequency (RF) carrier. The other is multicarrier modulation, where data is transmitted by simultaneously modulating multiple RF carriers. Multicarrier modulation is the principle of transmitting data by dividing the stream into several bit streams, each of which has a much lower bit rate, and by using these substreams to modulate several carriers.

In the first examples of multicarrier modulation the signal bandwidth was divided into several non-overlapping frequency subchannels, each modulated by a distinct stream of data coming from a common source. On one hand, the absence of any spectral overlap between adjacent subchannels helped to eliminate interference among different data streams (interchannel interference). On the other hand, it resulted into a very inefficient use of the available spectrum. These systems involved high hardware complexity since parallel data transmission was essentially implemented through a bank of oscillators, each tuned on a specific subcarrier.

OFDM is a multicarrier modulation technique where data symbols modulate a parallel collection of regularly spaced subcarriers. The subcarriers have the minimum frequency separation required to maintain orthogonality of their corresponding time domain waveforms, yet the signal spectra corresponding to the different subcarriers overlap in frequency. The spectral overlap results in a waveform that uses the available bandwidth with a very high bandwidth efficiency. The most important feature of OFDM is that, by choosing the subcarrier spacing properly in relation to the channel coherence bandwidth, it converts a frequency selective channel into a parallel collection of frequency flat subchannels. Hence, OFDM is a signaling technique that is widely adopted in many recently standardized broadband communication systems, due to its ability to cope with frequency selective fading.

# Chapter 2

## OFDM Structure

### 2.1 OFDM Transmitter

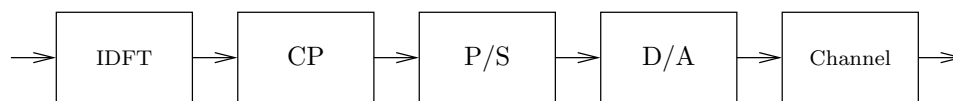


Figure 2.1: OFDM Transmitter.

#### 2.1.1 Signal Representation and Orthogonality

The “orthogonal” part of the OFDM name indicates that there is a precise mathematical relationship between the frequencies of the carriers in the system. As we have mentioned, in a normal FDM system the carriers are spaced apart in such way that the signals can be received using conventional filters and demodulators. In such receivers, guard bands have to be introduced between the different carriers, and the introduction of these guard bands in the frequency domain results in low spectral efficiency.

It is possible, however, to arrange the carriers in an OFDM signal so that the sidebands of the individual carriers overlap but the signals can still be received without adjacent

carrier interference. In order to do this, the carriers must be orthogonal. The receiver acts as a bank of demodulators, translating each carrier down to DC, the resulting signal then being integrated over a symbol period to recover the data.

The OFDM signal can be expressed as

$$s(t) = \sum_{k=0}^{N-1} s_k e^{j2\pi(f_o+k\Delta f)t}, \text{ for } 0 \leq t \leq T_s, \quad (2.1)$$

where  $s_k$  is the  $k$ -th transmitted symbol,  $\Delta f$  is the subcarrier spacing,  $T_s$  the OFDM symbol duration and  $N$  the number of symbols. Each symbol is tuned on a specific subcarrier and is orthogonal to each other, as can be shown below

$$\begin{aligned} & \frac{1}{T_s} \int_0^{T_s} e^{j2\pi(f_o+k\Delta f)t} e^{-j2\pi(f_o+l\Delta f)t} dt \\ &= \frac{1}{T_s} \int_0^{T_s} e^{j2\pi(k-l)\Delta f t} dt \\ &= \delta[k-l], \end{aligned} \quad (2.2)$$

where  $\delta[k]$  is the delta function and  $T_s\Delta f = 1$ . Using this property, the OFDM signal can be demodulated by

$$\begin{aligned} & \frac{1}{T_s} \int_0^{T_s} s(t) e^{-j2\pi(f_o+k\Delta f)t} dt \\ &= \frac{1}{T_s} \int_0^{T_s} \left( \sum_{l=0}^{N-1} s_l e^{j2\pi(f_o+l\Delta f)t} \right) e^{-j2\pi(f_o+k\Delta f)t} dt \\ &= \sum_{l=0}^{N-1} s_l \delta[l-k] \\ &= s_k. \end{aligned} \quad (2.3)$$

In order to avoid a large number of modulators and filters at the transmitter and comple-

mentary filters and demodulators at the receiver, it is desirable to be able to use digital signal processing techniques, such as Discrete Fourier Transform (DFT). The sinusoids of the DFT form an orthogonal basis set, and a signal in the vector space of the DFT can be represented as a linear combination of the orthogonal sinusoids. The OFDM transmitter can be implemented using the IDFT and the receiver using DFT.

The OFDM signal can be expressed as

$$s(t) = \sum_{k=0}^{N-1} s_k e^{j2\pi(f_o+k\Delta f)t}, \text{ for } 0 \leq t \leq T_s. \quad (2.4)$$

By modulating the original data onto  $N$  subcarriers, OFDM increases the symbol duration by a factor of  $N$ , thereby making the transmitted signal more robust against frequency selective fading. It is convenient to sample over the period of one data symbol, which is  $T = \frac{T_s}{N}$ . If the signal is sampled at  $t = n\frac{T_s}{N}$ , for  $n = 0, \dots, N-1$ , then the resulting signal is represented by

$$S_n = s\left(n\frac{T_s}{N}\right) = \sum_{k=0}^{N-1} s_k e^{j2\pi(f_o+k\Delta f)n\frac{T_s}{N}} \quad (2.5)$$

and, without loss of generality, by letting  $f_o = 0$ , the signal becomes

$$S_n = s\left(n\frac{T_s}{N}\right) = \sum_{k=0}^{N-1} s_k e^{j2\pi k\Delta f n\frac{T_s}{N}}, \quad (2.6)$$

where  $\Delta f = \frac{1}{T_s}$ . If we now simplify

$$S_n = s\left(n\frac{T_s}{N}\right) = \sum_{k=0}^{N-1} s_k e^{j\frac{2\pi kn}{N}}. \quad (2.7)$$

Therefore, using IDFT, the signal can be expressed as

$$S_n = \sum_{k=0}^{N-1} s_k e^{j\frac{2\pi kn}{N}} = \text{IDFT}(\mathbf{s})_n, \quad (2.8)$$

where  $\mathbf{s} = [s_0, \dots, s_{N-1}]^T$ . A general  $N$ -to- $N$  point linear transformation requires  $N^2$  multiplications and additions. This would be true for the DFT and IDFT. However, by calculating the output using the Fast Fourier Transform (FFT), we reduce the number of computations to the order of  $N \log N$ . The ability to define the signal in the frequency domain and to generate the signal using the Inverse Fast Fourier Transform is the key that has permitted OFDM to be developed as far as it has.

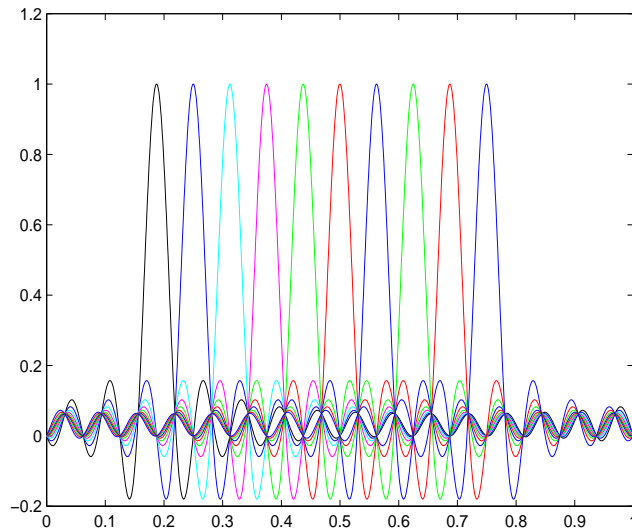


Figure 2.2: Orthogonality of the subcarriers.

### 2.1.2 Cyclic Prefix

A major problem in most wireless systems is the presence of a frequency-selective channel. The frequency selectivity destroys the orthogonality between the subcarriers. Furthermore,

multiple delayed versions of the transmitted signal arrive at the receiver. As a result, the multiple versions of the signal cause the received signal to be distorted. Data transmission in OFDM systems is accomplished in a block-wise fashion, where each block conveys a number  $N$  of data symbols. The received OFDM block is distorted by the previously transmitted OFDM block. This phenomenon results into interblock interference (IBI).

As a consequence of the frequency selective channel, blocks may partially overlap in the time domain. The common approach to mitigate IBI is to introduce a guard interval of appropriate length among adjacent blocks. The insertion of a silent guard period between successive OFDM blocks would avoid IBI, but it does not avoid the loss of the subcarrier orthogonality. In practice, the guard interval is obtained by duplicating the last  $N_g$  samples of each IDFT output and for this reason is referred to as cyclic prefix. The cyclic prefix is appended in front of the corresponding IDFT output. This results to an extended block of  $N_T = N + N_g$  samples which can totally remove the IBI as long as  $N_g$  is greater than the length of the channel impulse response. Assuming a time invariant frequency selective channel with discrete time impulse response  $\mathbf{h} = [h_0, h_1, \dots, h_{L-1}]^T$ , the length of the cyclic prefix  $N_g$  must be at least  $L$ .

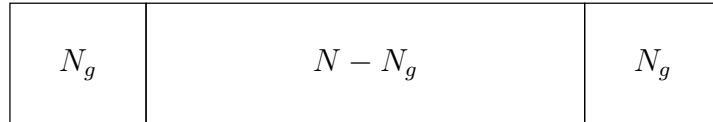


Figure 2.3: Structure of an OFDM block with CP insertion.

The output of the IDFT operation is denoted by  $\mathbf{S} = [S_0, S_1, \dots, S_{N-1}]^T$ . The cyclically extended block, which will be the input to the channel, is denoted by

$$\mathbf{x} = [S_{N-L+1}, S_{N-L+2}, \dots, S_{N-1}, S_0, S_1, \dots, S_{N-1}]^T. \quad (2.9)$$

## 2.2 OFDM Receiver

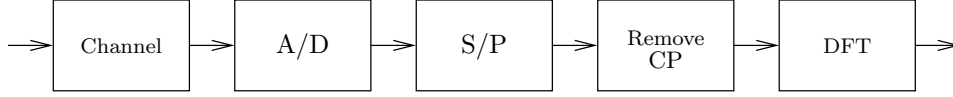


Figure 2.4: OFDM Receiver.

For the sake of simplicity, ideal timing and frequency synchronization is considered throughout this chapter. The receiver operations are essentially the reverse of those in the transmitter. By removing the cyclic prefix, which now contains IBI, an  $N$  point sequence is fed to the FFT unit for frequency domain transformation. The output of the FFT are the symbols modulated on the  $N$  subcarriers, each multiplied by a complex channel gain.

As we have mentioned above, the transmitted symbols are

$$\mathbf{x} = [S_{N-L+1}, S_{N-L+2}, \dots, S_{N-1}, S_0, S_1, \dots, S_{N-1}]^T. \quad (2.10)$$

The transmitted baseband OFDM signal that will pass through the channel is

$$x(t) = \sum_k x_k g(t - kT), \quad (2.11)$$

where  $g(t)$  is the pulse shaping filter. We assume that the continuous time channel is

$$c(t) = \sum_l c_l \delta(t - \tau_l). \quad (2.12)$$

The received signal can be expressed as

$$\begin{aligned}
y(t) &= x(t) * c(t) & (2.13) \\
&= x(t) * \sum_l c_l \delta(t - \tau_l) \\
&= \sum_l c_l x(t - \tau_l) \\
&= \sum_l c_l \sum_k x_k g(t - \tau_l - kT) \\
&= \sum_k x_k \sum_l c_l g(t - \tau_l - kT).
\end{aligned}$$

If the signal is sampled at  $mT$ ,

$$y_m = y(mT) = \sum_k x_k \sum_l c_l g(mT - \tau_l - kT). \quad (2.14)$$

Setting  $i = m - k$  we get

$$y_m = y(mT) = \sum_i x_{m-i} \sum_l c_l g(iT - \tau_l). \quad (2.15)$$

By defining  $h_i = \sum_l c_l g(iT - \tau_l)$ , we get

$$y_m = \sum_i h_i x_{m-i}. \quad (2.16)$$

Thus, the discrete time baseband equivalent model with the additive white gaussian noise is expressed as

$$y_m = \sum_{l=0}^{L-1} h_l x_{m-l} + w_m, \quad m = 1, \dots, N + L - 1, \quad (2.17)$$

where  $w_m$  is the low-pass filtered noise at the sampling instant  $mT$ , which is a  $\mathcal{CN}(0, \sigma_w^2)$  random variable. The IBI extends over the first  $L - 1$  symbols and the receiver ignores it

by considering only the output over the time interval  $m \in [L, N + L - 1]$ . Over this time interval, denoting

$$\mathbf{y} = [y_L, \dots, y_{N+L-1}]^T, \quad (2.18)$$

and the channel by a vector of length  $N$

$$\mathbf{h} = [h_0, h_1, \dots, h_{L-1}, 0, \dots, 0]^T, \quad (2.19)$$

the output can be written as

$$\mathbf{y} = \mathbf{h} \otimes \mathbf{S} + \mathbf{w}, \quad (2.20)$$

where  $\otimes$  denotes the cyclic convolution. Thus, the linear convolution of a frequency selective multipath channel has been transformed to a circular convolution. Ignoring the noise and taking the Discrete Fourier Transform, we get in the frequency domain

$$Y_k = \text{DFT}(\mathbf{y})_k = \text{DFT}(\mathbf{h} \otimes \mathbf{S})_k = \text{DFT}(\mathbf{h})_k \cdot \text{DFT}(\mathbf{S})_k = H_k \cdot s_k, \quad (2.21)$$

where  $\mathbf{s}$  is the Discrete Fourier Transform of  $\mathbf{S}$  and

$$H_k = \sum_{l=0}^{L-1} h_l e^{j \frac{2\pi k l}{N}}, \quad \text{for } k = 0, \dots, N - 1, \quad (2.22)$$

which is the frequency response of the channel at the  $k_{\text{th}}$  subchannel. Thus, a frequency-selective channel has been converted into  $N$  parallel frequency-flat channels, thereby simplifying the receiver design. Each symbol is multiplied by a channel gain, the received signal is similar to the original signal except that  $H_k s_k$  modulates the  $k_{\text{th}}$  subcarrier instead of  $s_k$ .

# Chapter 3

## Channel Estimation

In OFDM transmissions, the effect of channel distortion on each subcarrier is represented by a single complex-valued coefficient that affects the amplitude and phase of the relevant information symbol. Detection of the transmitted symbols can be performed only after channel equalization and can be accomplished in the frequency domain if an estimate of the channel response is available at the receiver. One common approach to recover channel state information (CSI) is based on the periodic insertion of pilot symbols within the transmitted signals.

The channel is assumed time invariant over each OFDM block, but can vary from block to block. Under these assumptions, the output of the receive DFT unit is given by

$$Y_k = H_k s_k + W_k, \text{ for } k = 0, \dots, N - 1, \quad (3.1)$$

where  $H_k$  is the channel frequency response over the  $k_{\text{th}}$  subcarrier,  $s_k$  is the relevant data symbol and  $W_k$  represents the noise. One feature of OFDM is that channel equalization can independently be performed over each subcarrier. In practice, the  $k_{\text{th}}$  DFT output  $Y_k$  is weighted by a complex valued quantity  $\frac{1}{\hat{H}_k}$  in an attempt to compensate for the channel

attenuation and phase rotation. The equalized sample  $\hat{Y}_k = \frac{Y_k}{\hat{H}_k}$  is subsequently passed to the detection unit, which delivers the final decisions  $\hat{s}_k$  on the transmitted data.

A popular approach for the estimation of the channel impulse response is Least Squares Estimation. The received samples corresponding to the pilot symbols can be expressed as

$$Y_n = H_n s_n + W_n, \quad n \in \mathcal{I}, \quad (3.2)$$

where  $\mathcal{I}$  denotes the set of subcarriers on which pilot symbols are transmitted. The channel impulse response of the frequency selective channel is denoted as

$$\mathbf{h} = [h_0, h_1, \dots, h_{L-1}]^T, \quad (3.3)$$

where  $L$  denotes the number of taps. By defining the  $L \times N$  matrix  $\mathbf{F}$ , with  $(l, n)$ -th element

$$[\mathbf{F}]_{l,n} := e^{\frac{j2\pi(l-1)(n-1)}{N}}, \quad (3.4)$$

and let  $\mathbf{f}_n$  be the  $n$ -th column of  $\mathbf{F}$ , then

$$H_n = \mathbf{f}_n^H \mathbf{h}. \quad (3.5)$$

Suppose that the set of pilot subcarriers is given by  $\mathcal{I} = \{n_1, \dots, n_p\}$ . Letting

$$\tilde{\mathbf{H}} := [H_{n_1}, \dots, H_{n_p}]^T \quad (3.6)$$

contain the channel frequency response on pilot subcarriers and defining

$$\mathbf{F}_p := [\mathbf{f}_{n_1}, \dots, \mathbf{f}_{n_p}], \quad (3.7)$$

we can express the channel frequency response on the pilot subcarriers as

$$\tilde{\mathbf{H}} = \mathbf{F}_p^H \mathbf{h}. \quad (3.8)$$

Let the  $p \times 1$  vector  $\mathbf{y} = [y_{n_1}, \dots, y_{n_p}]^T$  consist of the received samples that correspond to the pilot symbols  $\mathbf{s} = [s_{n_1}, \dots, s_{n_p}]^T$ . Then,  $\mathbf{y}$  can be rewritten as

$$\mathbf{y} = \mathcal{D}(\mathbf{s})\tilde{\mathbf{H}} + \mathbf{w} = \mathcal{D}(\mathbf{s})\mathbf{F}_p^H \mathbf{h} + \mathbf{w}, \quad (3.9)$$

where  $\mathcal{D}(\mathbf{s})$  is a diagonal matrix with elements the pilot symbols.

From the above equation, we estimate the channel impulse response  $\mathbf{h}$ . The LS channel estimate is computed as

$$\hat{\mathbf{h}} = \arg \min_{\mathbf{h}} \|\mathbf{y} - \mathcal{D}(\mathbf{s})\mathbf{F}_p^H \mathbf{h}\|^2. \quad (3.10)$$

Thus, the channel estimate is given by

$$\hat{\mathbf{h}} = (\mathbf{F}_p \mathcal{D}(\mathbf{s})^H \mathcal{D}(\mathbf{s}) \mathbf{F}_p^H)^{-1} (\mathbf{F}_p \mathcal{D}(\mathbf{s})^H) \mathbf{y}, \quad (3.11)$$

and the estimated channel frequency response on the  $n$ -th subcarrier is

$$\hat{H}_n = \mathbf{f}_n^H \hat{\mathbf{h}}. \quad (3.12)$$

# Chapter 4

## Synchronization in OFDM systems

Synchronization plays a major role in the design of a digital communication system. In order to demodulate an OFDM signal, the OFDM receiver needs to perform two important synchronization tasks. The first is to identify the start of each received OFDM block so as to find the correct position of the DFT window. This is referred to as *time synchronization*. The second is to align its local carrier frequency as closely as possible to the transmitter carrier frequency. This is referred to as carrier *frequency synchronization*.

Symbol timing and Carrier Frequency Offset (CFO) estimation errors can significantly degrade the performance of OFDM systems. The symbol timing synchronization error may cause interblock interference (IBI). The frequency synchronization error is one of the sources of intercarrier interference (ICI). Carrier Frequency Offset degrades the orthogonality of the received signal, since the received samples of the DFT will contain interference from the adjacent subcarriers.

Compared with single-carrier systems, OFDM can tolerate larger errors in estimating the start of a symbol since the OFDM symbol structure accommodates a reasonable degree of time synchronization error, because of the cyclic prefix. On the other hand, frequency synchronization in OFDM must be tighter than that in single-carrier systems, due to the

narrowness of the OFDM subcarriers. The multicarrier signal is very sensitive to frequency offsets because it needs to retain the orthogonality between the subcarriers.

If the correct position of the DFT window has not been found, then the timing window will slide to the left or the right. As a consequence, a unique phase change will be introduced to each of the subcarriers,

$$s(t - \tau) \iff e^{-j\omega\tau} S(\omega). \quad (4.1)$$

However, if perfect synchronization is not maintained, it is still possible to tolerate a timing offset of  $\tau$  seconds without any degradation in performance, as long as

$$0 \leq \tau \leq T_h - T_g, \quad (4.2)$$

where  $T_g$  is the cyclic prefix duration and  $T_h$  is the maximum channel delay spread. As long as  $0 \leq \tau \leq T_h - T_g$ , the timing offset can be included by the channel estimator in the complex gain estimate for each subchannel, and the appropriate phase shift can be applied by the Frequency Domain Equalizer (FEQ).

In the frequency domain, if the carrier frequency synchronization is perfect, the receiver samples at the peak of each subcarrier, where the desired subcarrier amplitude is maximized, and the intercarrier interference (ICI) is zero. Since the zero crossings of the frequency domain sinc pulses all line up as seen in Figures 4.1 and 4.2, as long as the frequency offset  $\epsilon = 0$ , there is no interference between the subcarriers. One intuitive interpretation for this is that since the FFT is essentially a frequency-sampling operation, if the frequency offset is negligible, the receiver simply samples the received signal at the peak points of the sinc functions, where the ICI is zero from all the neighboring subcarriers.

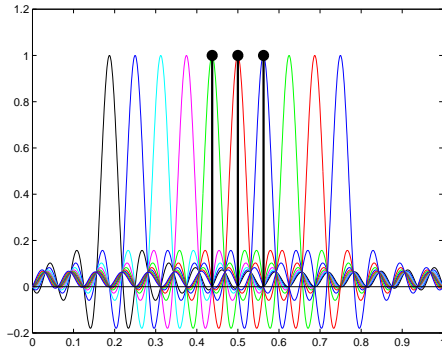


Figure 4.1: Without Frequency Offset,  $\epsilon = 0$ .

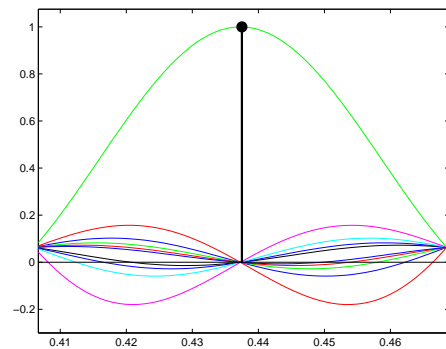


Figure 4.2: Zoom in, one subcarrier.

However, in practice, the frequency offset is not zero. The major causes for this are mismatched oscillators at the transmitter and the receiver and Doppler frequency shifts due to mobility. If the carrier frequency is misaligned by some amount  $\epsilon$ , some of the desired energy is lost, and more significantly, intercarrier interference is introduced. In the presence of frequency offset, the subcarriers overlap rather than having each subcarrier spectrally isolated.

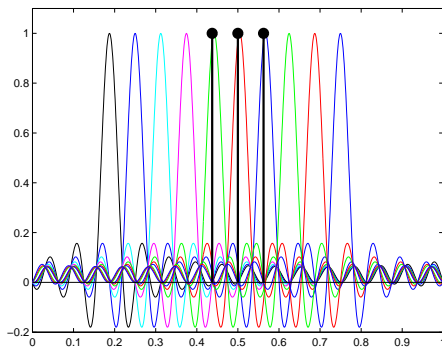


Figure 4.3: With Frequency Offset,  $\epsilon \neq 0$ .

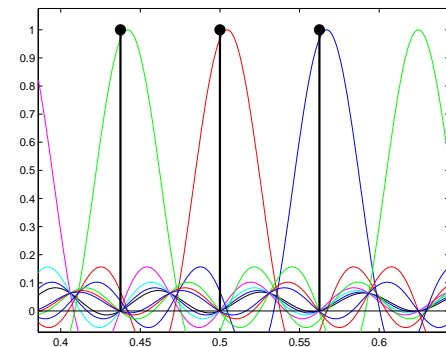


Figure 4.4: Zoom in.

## 4.1 Time Synchronization

### 4.1.1 Blind Method

A number of time synchronization algorithms in the OFDM systems have been proposed. Most of them are based on the correlation of identical parts of the OFDM symbol. The correlation between the cyclic prefix and the corresponding end of the OFDM symbol, or between two identical halves of the synchronization symbol. The transmitter inserts a

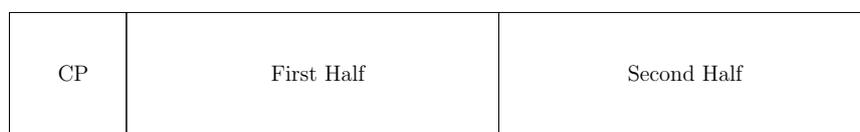


Figure 4.5: Structure of an OFDM synchronization symbol.

synchronization symbol at the beginning of a group of OFDM data symbols. Consider a pilot symbol preceded by CP as shown in Figure 4.5. In this pilot symbol, the second half is equal to the first half, excluding the cyclic prefix. This is equivalent to only using every other tone in the OFDM symbol, see Figure 4.6. This means that at each even frequency a symbol is transmitted. To ensure that the time-domain pilot signal has the same average energy as the data symbols, the energy on each used subchannel is doubled. If the length of CP is at least as large as that of the channel impulse response, then the two halves of the symbol remain identical at the output of the channel, except for a phase difference between them due to carrier frequency offset.

The two identical halves are placed at the start of the data symbols. The symbol timing is found by searching for a symbol in which the first half is identical to the second half in the time domain.

As we have mentioned in previous chapter, the output of the IDFT unit is denoted by

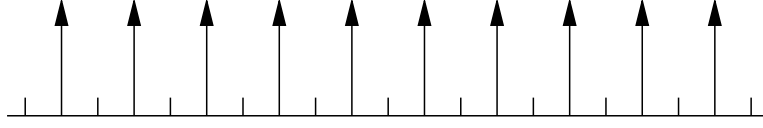


Figure 4.6: Frequency characteristics of synchronization symbol.

$\mathbf{S} = [S_0, S_1, \dots, S_{N-1}]^T$ , where

$$S_n = \frac{1}{\sqrt{N}} \sum_{k=0}^{N-1} s_k e^{j\frac{2\pi kn}{N}}, \quad (4.3)$$

and the transmitted symbols are

$$\mathbf{x} = [S_{N-L+1}, S_{N-L+2}, \dots, S_{N-1}, S_0, S_1, \dots, S_{N-1}]^T. \quad (4.4)$$

The signal is transmitted through a frequency selective multipath channel. The normalized carrier frequency offset can be written as  $\epsilon = \Delta F T$ , which causes a phase rotation of  $\frac{2\pi\epsilon n}{N}$ .

The received samples of the OFDM symbol are given by

$$y_n = e^{j\frac{2\pi\epsilon n}{N}} \sum_{l=0}^{L-1} h_l x_{n-l} + w_n. \quad (4.5)$$

Denoting

$$r_n = \sum_{l=0}^{L-1} h_l x_{n-l}, \quad (4.6)$$

then, the received samples can be expressed as

$$y_n = e^{j\frac{2\pi\epsilon n}{N}} r_n + w_n. \quad (4.7)$$

The transmitted training symbol is expressed as

$$\mathbf{x} = \left[ \underbrace{S_{\frac{N}{2}-L+1}, S_{\frac{N}{2}-L+2}, \dots, S_{\frac{N}{2}-1}}_{\text{CP}}, \underbrace{S_0, S_1, \dots, S_{\frac{N}{2}-1}}_{\text{First Half}}, \underbrace{S_0, S_1, \dots, S_{\frac{N}{2}-1}}_{\text{Second Half}} \right]^T. \quad (4.8)$$

At the receiver, we correlate the received signal  $y_{d+m+\frac{N}{2}}$  with  $y_{d+m}^*$  and compute

$$P(d) = \sum_{m=0}^{\frac{N}{2}-1} \left( y_{d+m}^* y_{d+m+\frac{N}{2}} \right), \quad (4.9)$$

where  $d$  is a time index corresponding to the first sample in a window of  $N$  samples. This window slides along in time as the receiver searches for the first training symbol. A symbol estimator is defined as

$$\hat{d} = \arg \max_d |P(d)|. \quad (4.10)$$

In the sequel, we prove that the correlation timing metric is a random variable, with constant mean value, when  $d$  is inside the cyclic prefix. When  $d$  is outside the cyclic prefix, the mean value of the timing metric is approximately zero because there is no useful signal and the correlation is between noise samples.

Assume an ideal noiseless channel. Then, the samples of the received training symbol are

$$y_n = e^{\frac{j2\pi\epsilon n}{N}} x_{(n-L) \bmod \frac{N}{2}}, \quad \text{for } n = 0, \dots, N + L - 1. \quad (4.11)$$

By multiplying the conjugate of one sample from first half with the corresponding sample from the second half, the sum of products is

$$\begin{aligned}
P(d) &= \sum_{m=0}^{\frac{N}{2}-1} \left( y_{d+m}^* y_{d+m+\frac{N}{2}} \right) \tag{4.12} \\
&= \sum_{m=0}^{\frac{N}{2}-1} \left( e^{\frac{j2\pi\epsilon(d+m)}{N}} x_{(d+m-L)\bmod\frac{N}{2}} \right)^* \left( e^{\frac{j2\pi\epsilon(d+m+\frac{N}{2})}{N}} x_{(d+m+\frac{N}{2}-L)\bmod\frac{N}{2}} \right) \\
&= \sum_{m=0}^{\frac{N}{2}-1} \left( e^{-\frac{j2\pi\epsilon(d+m)}{N}} x_{(d+m-L)\bmod\frac{N}{2}}^* e^{\frac{j2\pi\epsilon(d+m+\frac{N}{2})}{N}} x_{(d+m+\frac{N}{2}-L)\bmod\frac{N}{2}} \right) \\
&= \sum_{m=0}^{\frac{N}{2}-1} \left( e^{j\pi\epsilon} x_{(d+m-L)\bmod\frac{N}{2}}^* x_{(d+m+\frac{N}{2}-L)\bmod\frac{N}{2}} \right) \\
&= e^{j\pi\epsilon} \sum_{m=0}^{\frac{N}{2}-1} \left( x_{(d+m-L)\bmod\frac{N}{2}}^* x_{(d+m+\frac{N}{2}-L)\bmod\frac{N}{2}} \right).
\end{aligned}$$

If  $d$  corresponds to a sample in the interval of the cyclic prefix, then

$$x_{(d+m-L)\bmod\frac{N}{2}} = x_{(d+m+\frac{N}{2}-L)\bmod\frac{N}{2}}, \text{ for } m = 0, \dots, \frac{N}{2} - 1. \tag{4.13}$$

As a consequence

$$\begin{aligned}
P(d) &= \sum_{m=0}^{\frac{N}{2}-1} \left( y_{d+m}^* y_{d+m+\frac{N}{2}} \right) \tag{4.14} \\
&= e^{j\pi\epsilon} \sum_{m=0}^{\frac{N}{2}-1} \left( x_{(d+m-L)\bmod\frac{N}{2}}^* x_{(d+m+\frac{N}{2}-L)\bmod\frac{N}{2}} \right) \\
&= e^{j\pi\epsilon} \sum_{m=0}^{\frac{N}{2}-1} \left( \left| x_{(d+m-L)\bmod\frac{N}{2}} \right|^2 \right).
\end{aligned}$$

It is important to note that the carrier frequency offset does not affect the timing metric

$$|P(d)| = \sum_{m=0}^{\frac{N}{2}-1} \left( \left| x_{(d+m-L)\bmod\frac{N}{2}} \right|^2 \right), \text{ for } 0 \leq d \leq L. \tag{4.15}$$

Because of the structure of the training symbol, for  $L \leq d \leq L + \frac{N}{2}$

$$\begin{cases} x_{(d+m-L) \bmod \frac{N}{2}} = x_{(d+m+\frac{N}{2}-L) \bmod \frac{N}{2}}, & \text{for } m = 0, \dots, \frac{N}{2} - d - 1 \\ x_{(d+m-L) \bmod \frac{N}{2}} \neq x_{(d+m+\frac{N}{2}-L) \bmod \frac{N}{2}}, & \text{for } m = \frac{N}{2} - d, \dots, \frac{N}{2} - 1. \end{cases}$$

Let  $d_*$  is a sample in the interval of the cyclic prefix. Then, the following relation is satisfied

$$|P(d)| < |P(d_*)|, \text{ for } d > L. \quad (4.16)$$

For large  $N$ , the output of the IDFT unit can be treated as independent zero-mean complex

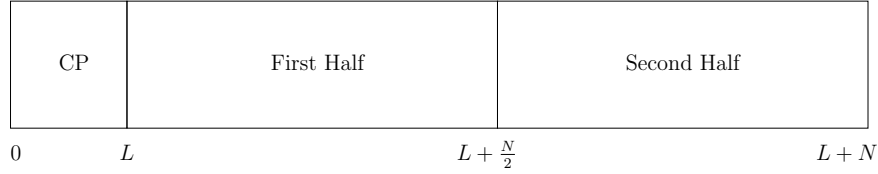


Figure 4.7: Structure of an OFDM synchronization symbol.

gaussian random variables with variance  $\sigma_x^2$ . We compute the mean value of  $|P(d)|$

- For  $0 \leq d \leq L$ ,

$$\begin{aligned} E[|P(d)|] &= E \left[ \sum_{m=0}^{\frac{N}{2}-1} \left( |x_{(d+m-L) \bmod \frac{N}{2}}|^2 \right) \right] \\ &= \frac{N}{2} E[|x|^2] \\ &= \frac{N}{2} \sigma_x^2. \end{aligned} \quad (4.17)$$

- For  $L < d \leq L + \frac{N}{2}$ , we have mentioned that

$$\begin{cases} x_{(d+m-L) \bmod \frac{N}{2}} = x_{(d+m+\frac{N}{2}-L) \bmod \frac{N}{2}}, & \text{for } m = 0, \dots, \frac{N}{2} - d - 1 \\ x_{(d+m-L) \bmod \frac{N}{2}} \neq x_{(d+m+\frac{N}{2}-L) \bmod \frac{N}{2}}, & \text{for } m = \frac{N}{2} - d, \dots, \frac{N}{2} - 1. \end{cases}$$

Then,

$$\begin{aligned}
E [|P(d)|] &= E \left[ \sum_{m=0}^{\frac{N}{2}-1} \left( x_{(d+m-L) \bmod \frac{N}{2}}^* x_{(d+m+\frac{N}{2}-L) \bmod \frac{N}{2}} \right) \right] \quad (4.18) \\
&= E \left[ \sum_{m=0}^{\frac{N}{2}-d-1} \left( x_{(d+m-L) \bmod \frac{N}{2}}^* x_{(d+m+\frac{N}{2}-L) \bmod \frac{N}{2}} \right) \right. \\
&\quad \left. + \sum_{m=\frac{N}{2}-d}^{\frac{N}{2}-1} \left( x_{(d+m-L) \bmod \frac{N}{2}}^* x_{(d+m+\frac{N}{2}-L) \bmod \frac{N}{2}} \right) \right] \\
&= \left[ \sum_{m=\frac{N}{2}-d}^{\frac{N}{2}-1} E \left[ x_{(d+m-L) \bmod \frac{N}{2}}^* \right] E \left[ x_{(d+m+\frac{N}{2}-L) \bmod \frac{N}{2}} \right] \right] + \left( \frac{N}{2} - d \right) \sigma_x^2 \\
&= \left( \frac{N}{2} - d \right) \sigma_x^2.
\end{aligned}$$

- For  $d > L + \frac{N}{2}$ ,

$$\begin{aligned}
E [|P(d)|] &= E \left[ \sum_{m=0}^{\frac{N}{2}-1} \left( x_{(d+m-L) \bmod \frac{N}{2}}^* x_{(d+m+\frac{N}{2}-L) \bmod \frac{N}{2}} \right) \right] \quad (4.19) \\
&= \sum_{m=0}^{\frac{N}{2}-1} \left( E \left[ x_{(d+m-L) \bmod \frac{N}{2}}^* \right] E \left[ x_{(d+m+\frac{N}{2}-L) \bmod \frac{N}{2}} \right] \right) \\
&= 0.
\end{aligned}$$

Assuming that the transmission channel is flat fading, the timing metric reaches a plateau (Figure 4.8) which has a length equal to the length of the guard interval, since there is no ISI within this plateau to distort the signal. On the contrary, for frequency selective channels (Figure 4.9), the length of the plateau will have a length equal to the length of the guard interval minus the length of the channel impulse response since there will be ISI which will distort the cyclic prefix.

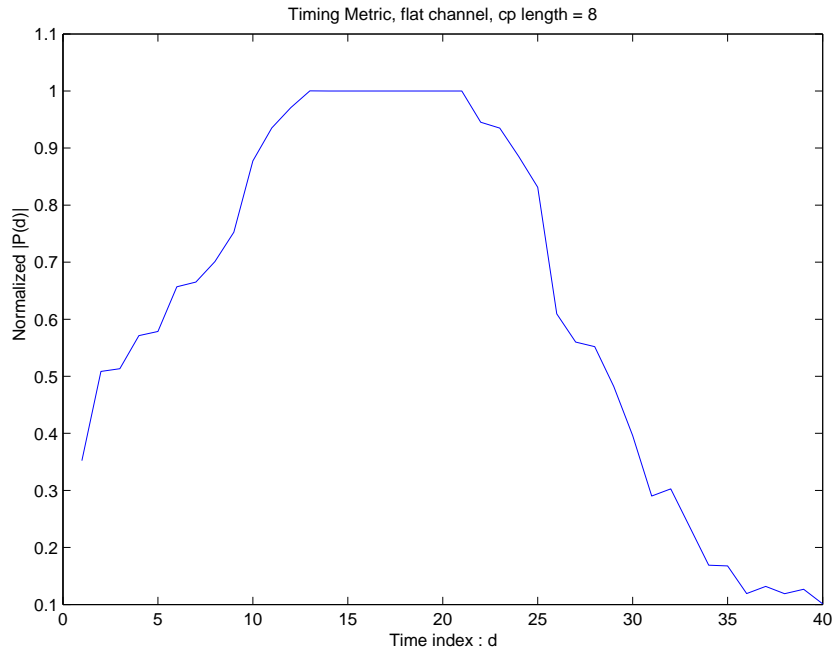


Figure 4.8: Timing Metric - Blind Method, Flat Channel.

A drawback of the above timing metric is the flat region (plateau), due to the cyclic prefix. This estimator provides useful information about the start of the packet, but not for the perfect symbol timing synchronization. The plateau causes some ambiguity in determining the correct timing index. It is possible to start sampling anywhere in the plateau.

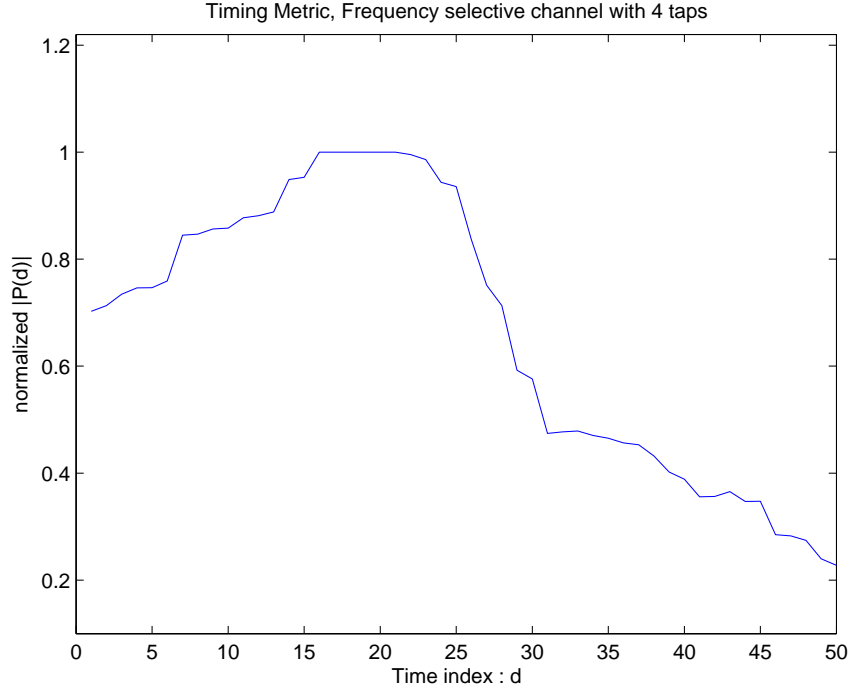


Figure 4.9: Timing Metric - Blind Method, Frequency Selective Channel.

### 4.1.2 Pilot Based Method

In order to avoid the plateau of the previous correlation timing metric, it will be presented another timing metric which also exploits the structure of the training symbol, but in a different way. The receiver has complete knowledge of the training symbol and uses the first-half (or the second-half) of the training symbol. We have mentioned that the transmitted training symbol is expressed as

$$\mathbf{x} = \left[ S_{\frac{N}{2}-L+1}, S_{\frac{N}{2}-L+2}, \dots, S_{\frac{N}{2}-1}, S_0, S_1, \dots, S_{\frac{N}{2}-1}, S_0, S_1, \dots, S_{\frac{N}{2}-1} \right]^T. \quad (4.20)$$

By defining

$$\mathbf{a} = \left[ S_0, S_1, \dots, S_{\frac{N}{2}-1} \right]^T, \quad (4.21)$$

we get

$$\mathbf{x} = \left[ S_{\frac{N}{2}-L+1}, S_{\frac{N}{2}-L+2}, \dots, S_{\frac{N}{2}-1}, \mathbf{a}^T, \mathbf{a}^T \right]^T. \quad (4.22)$$

At the receiver, not only a correlation is performed but also a multiplication with the training sequence  $\mathbf{a} = [S_0, S_1, \dots, S_{\frac{N}{2}-1}]^T$ . As a consequence, the sum of the pairs of products will be

$$P(d) = \sum_{m=0}^{\frac{N}{2}-1} \left( y_{d+m} \mathbf{a}_m \right)^* \left( y_{d+m+\frac{N}{2}} \mathbf{a}_m \right). \quad (4.23)$$

Assume an ideal channel with no noise and that the received samples of the training symbol are

$$y_n = e^{\frac{j2\pi\epsilon n}{N}} x_{(n-L) \bmod \frac{N}{2}}, \text{ for } n = 0, \dots, N+L-1. \quad (4.24)$$

Then,

$$\begin{aligned} P(d) &= \sum_{m=0}^{\frac{N}{2}-1} \left( y_{d+m} \mathbf{a}_m \right)^* \left( y_{d+m+\frac{N}{2}} \mathbf{a}_m \right) \\ &= \sum_{m=0}^{\frac{N}{2}-1} \left( e^{\frac{j2\pi\epsilon(d+m)}{N}} x_{(d+m-L) \bmod \frac{N}{2}} \mathbf{a}_m \right)^* \left( e^{\frac{j2\pi\epsilon(d+m+\frac{N}{2})}{N}} x_{(d+m+\frac{N}{2}-L) \bmod \frac{N}{2}} \mathbf{a}_m \right) \\ &= \sum_{m=0}^{\frac{N}{2}-1} \left( e^{-\frac{j2\pi\epsilon(d+m)}{N}} x_{(d+m-L) \bmod \frac{N}{2}}^* \mathbf{a}_m^* e^{\frac{j2\pi\epsilon(d+m+\frac{N}{2})}{N}} x_{(d+m+\frac{N}{2}-L) \bmod \frac{N}{2}} \mathbf{a}_m \right) \\ &= \sum_{m=0}^{\frac{N}{2}-1} \left( e^{j\pi\epsilon} x_{(d+m-L) \bmod \frac{N}{2}}^* x_{(d+m+\frac{N}{2}-L) \bmod \frac{N}{2}} |\mathbf{a}_m|^2 \right) \\ &= e^{j\pi\epsilon} \sum_{m=0}^{\frac{N}{2}-1} \left( x_{(d+m-L) \bmod \frac{N}{2}}^* x_{(d+m+\frac{N}{2}-L) \bmod \frac{N}{2}} |\mathbf{a}_m|^2 \right). \end{aligned} \quad (4.25)$$

If  $d$  corresponds to a sample in the interval of the cyclic prefix, then

$$x_{(d+m-L)\bmod\frac{N}{2}} = x_{(d+m+\frac{N}{2}-L)\bmod\frac{N}{2}}, \quad \text{for } m = 0, \dots, \frac{N}{2} - 1, \quad (4.26)$$

and also

$$x_{(d+m-L)\bmod\frac{N}{2}} \neq a_m, \quad \text{for } m = 0, \dots, \frac{N}{2} - 1. \quad (4.27)$$

Then,

$$\begin{aligned} P(d) &= \sum_{m=0}^{\frac{N}{2}-1} \left( y_{d+m} a_m \right)^* \left( y_{d+m+\frac{N}{2}} a_m \right) \\ &= e^{j\pi\epsilon} \sum_{m=0}^{\frac{N}{2}-1} \left( x_{(d+m-L)\bmod\frac{N}{2}}^* x_{(d+m+\frac{N}{2}-L)\bmod\frac{N}{2}} |a_m|^2 \right) \\ &= e^{j\pi\epsilon} \sum_{m=0}^{\frac{N}{2}-1} \left( \left| x_{(d+m-L)\bmod\frac{N}{2}} \right|^2 |a_m|^2 \right). \end{aligned} \quad (4.28)$$

Computing the magnitude of  $P(d)$ , the carrier frequency offset does not affect the timing metric

$$|P(d)| = \sum_{m=0}^{\frac{N}{2}-1} \left( \left| x_{(d+m-L)\bmod\frac{N}{2}} \right|^2 |a_m|^2 \right), \quad \text{for } 0 \leq d \leq L. \quad (4.29)$$

The symbols at the output of the IDFT unit can be treated as zero-mean complex-valued gaussian random variables. As a consequence,  $x$  and  $a$  are independent zero-mean complex gaussian random variables with variance  $\sigma_x^2$  and  $\sigma_a^2$  respectively. We compute the mean value of  $|P(d)|$ .

- For  $0 \leq d < L$ ,

$$\begin{aligned}
E [|P(d)|] &= E \left[ \sum_{m=0}^{\frac{N}{2}-1} \left( |x_{(d+m-L) \bmod \frac{N}{2}}|^2 |a_m|^2 \right) \right] \\
&= \frac{N}{2} E [|x|^2 |a|^2] = \frac{N}{2} E [|x|^2] E [|a|^2] \\
&= \frac{N}{2} \sigma_x^2 \sigma_a^2.
\end{aligned} \tag{4.30}$$

- For  $L < d \leq L + \frac{N}{2}$ ,

$$\begin{aligned}
E [|P(d)|] &= E \left[ \sum_{m=0}^{\frac{N}{2}-1} \left( x_{(d+m-L) \bmod \frac{N}{2}}^* x_{(d+m+\frac{N}{2}-L) \bmod \frac{N}{2}} |a_m|^2 \right) \right] \\
&= E \left[ \sum_{m=0}^{\frac{N}{2}-d-1} \left( x_{(d+m-L) \bmod \frac{N}{2}}^* x_{(d+m+\frac{N}{2}-L) \bmod \frac{N}{2}} |a_m|^2 \right) \right. \\
&\quad \left. + \sum_{m=\frac{N}{2}-d}^{\frac{N}{2}-1} \left( x_{(d+m-L) \bmod \frac{N}{2}}^* x_{(d+m+\frac{N}{2}-L) \bmod \frac{N}{2}} |a_m|^2 \right) \right] \\
&= \left[ \sum_{m=\frac{N}{2}-d}^{\frac{N}{2}-1} E \left[ x_{(d+m-L) \bmod \frac{N}{2}}^* \right] E \left[ x_{(d+m+\frac{N}{2}-L) \bmod \frac{N}{2}} \right] E [|a_m|^2] \right] + \left( \frac{N}{2} - d \right) \sigma_x^2 \sigma_a^2 \\
&= \left( \frac{N}{2} - d \right) \sigma_x^2 \sigma_a^2.
\end{aligned} \tag{4.31}$$

- For  $d = d_*$ , which is the correct symbol timing, we note that

$$x_{(d+m-L) \bmod \frac{N}{2}} = x_{(d+m+\frac{N}{2}-L) \bmod \frac{N}{2}} = a_m, \quad \text{for } m = 0, \dots, \frac{N}{2} - 1. \tag{4.32}$$

Thus,

$$\begin{aligned}
|P(d)| &= \sum_{m=0}^{\frac{N}{2}-1} \left( \left| x_{(d+m-L) \bmod \frac{N}{2}} \right|^2 |a_m|^2 \right) \\
&= \sum_{m=0}^{\frac{N}{2}-1} |a_m|^4.
\end{aligned} \tag{4.33}$$

In the mean, the timing metric at the correct symbol timing,  $d_*$ , will be <sup>1</sup>

$$\begin{aligned}
E [|P(d_*)|] &= E \left[ \sum_{m=0}^{\frac{N}{2}-1} |a_m|^4 \right] = \sum_{m=0}^{\frac{N}{2}-1} E [|a_m|^4] \\
&= \sum_{m=0}^{\frac{N}{2}-1} 2\sigma_a^4 = N\sigma_a^4.
\end{aligned} \tag{4.34}$$

We have shown that

$$E [|P(d)|] = \begin{cases} \frac{N}{2} \sigma_x^2 \sigma_a^2, & \text{for } 0 \leq d < L, \\ N\sigma_a^4, & \text{for } d = d_*, \\ (\frac{N}{2} - d) \sigma_x^2 \sigma_a^2, & \text{for } L < d \leq L + \frac{N}{2}, \end{cases}$$

where  $\sigma_x^2 = \sigma_a^2$ .  $a$  and  $x$  are independent random variables, having the same distribution,  $\mathcal{CN}(0, \sigma_a^2)$ . As a consequence,

$$\frac{E [|P(d)|]}{N/2} = \begin{cases} \sigma_a^4, & \text{for } 0 \leq d < L \\ 2\sigma_a^4, & \text{for } d = d_* \\ (1 - \frac{2d}{N}) \sigma_a^4, & \text{for } L < d \leq L + \frac{N}{2}. \end{cases}$$

---

<sup>1</sup>see Appendix 4A for the computation of the fourth order moment

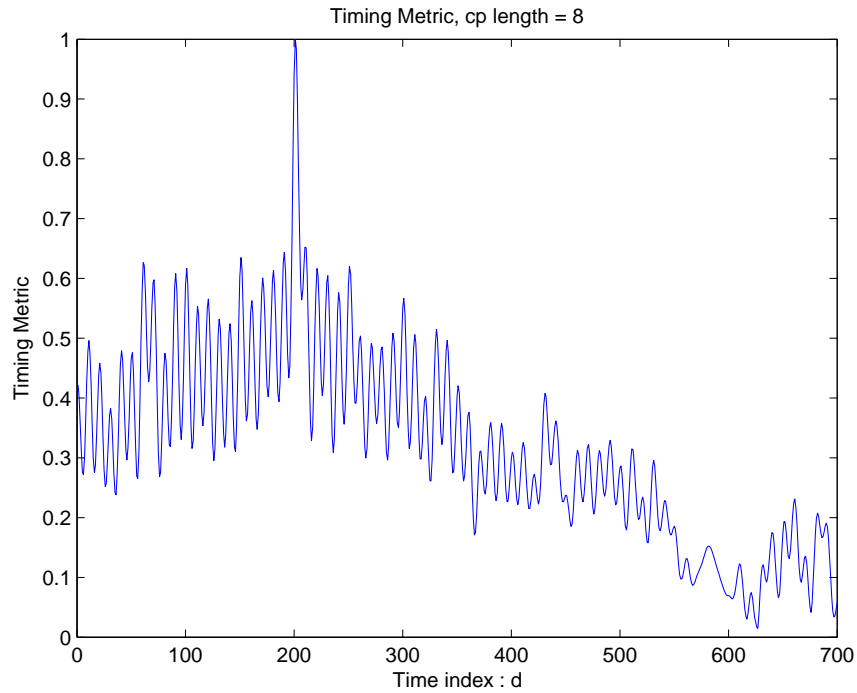


Figure 4.10: Timing Metric - Pilot Based Method.

Figure 4.10 verifies the above results for the pilot based timing metric. The peak of the normalized timing metric shows the correct symbol timing. For  $0 \leq d < L$ , the value of the timing metric is approximately the half of the value of the peak and for  $L < d \leq L + \frac{N}{2}$  is continuously decreased.

Figures 4.11 and 4.12 show the histogram of the pilot based method, for SNR = 0dB and SNR=10dB respectively. The correct timing index  $d$  is  $d_* = 201$ .

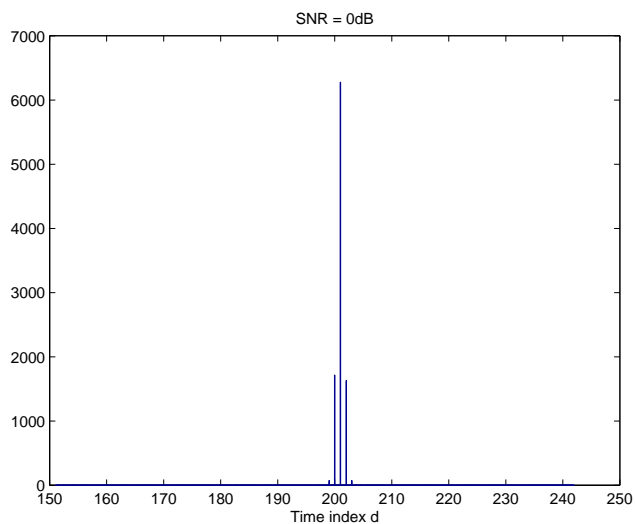


Figure 4.11: Histogram of  $d_*$ , 10000 iterations, SNR = 0dB.

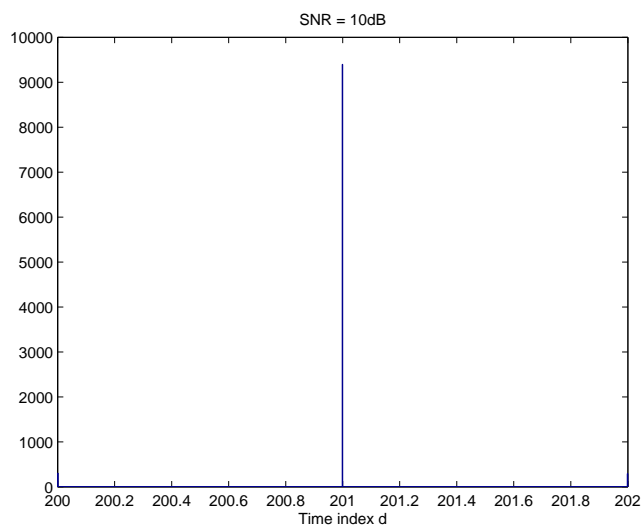


Figure 4.12: Histogram of  $d_*$ , 10000 iterations, SNR = 10dB.

### 4.1.3 First and second order statistics of the pilot based metric

In the previous chapters, we had assumed an ideal noiseless channel. In order to analyze the pilot based metric, we have to deal with the received signal

$$y_n = s_n + w_n, \text{ for } n = 0, \dots, N + L - 1, \quad (4.35)$$

where  $w_n$  is white complex gaussian noise,  $w_n \sim \mathcal{CN}(0, \sigma_w^2)$ . The pilot based timing metric scaled by  $M = \frac{N}{2}$  can be expressed as

$$\begin{aligned} T(d) &= \frac{1}{M} \sum_{m=0}^{M-1} \left( y_{d+m} \mathbf{a}_m \right)^* \left( y_{d+m+M} \mathbf{a}_m \right) \\ &= \frac{1}{M} \sum_{m=0}^{M-1} \left( (s_{d+m} + w_{d+m}) \mathbf{a}_m \right)^* \left( (s_{d+m+M} + w_{d+m+M}) \mathbf{a}_m \right) \\ &= \frac{1}{M} \sum_{m=0}^{M-1} \left( s_{d+m} \mathbf{a}_m + w_{d+m} \mathbf{a}_m \right)^* \left( s_{d+m+M} \mathbf{a}_m + w_{d+m+M} \mathbf{a}_m \right) \\ &= \frac{1}{M} \sum_{m=0}^{M-1} \left( s_{d+m}^* \mathbf{a}_m^* + w_{d+m}^* \mathbf{a}_m^* \right) \left( s_{d+m+M} \mathbf{a}_m + w_{d+m+M} \mathbf{a}_m \right) \\ &= \frac{1}{M} \sum_{m=0}^{M-1} \left( s_{d+m}^* s_{d+m+M} |\mathbf{a}_m|^2 + s_{d+m}^* w_{d+m+M} |\mathbf{a}_m|^2 \right. \\ &\quad \left. + w_{d+m}^* s_{d+m+M} |\mathbf{a}_m|^2 + w_{d+m}^* w_{d+m+M} |\mathbf{a}_m|^2 \right). \end{aligned} \quad (4.36)$$

If  $d$  corresponds to a sample in the interval of the cyclic prefix,  $0 \leq d < L$ , then

$$s_{d+m} = s_{d+m+M}, \text{ for } m = 0, \dots, M - 1. \quad (4.37)$$

By defining

$$r_m := s_{d+m}, \quad w_{1,m} := w_{d+m}, \quad w_{2,m} := w_{d+m+M}, \quad (4.38)$$

where  $r_m \sim \mathcal{CN}(0, \sigma_r^2)$ ,  $w_{1,m} \sim \mathcal{CN}(0, \sigma_w^2)$  and  $w_{2,m} \sim \mathcal{CN}(0, \sigma_w^2)$ , we get

$$\begin{aligned} T(d) &= \frac{1}{M} \sum_{m=0}^{M-1} \left( y_{d+m} \mathbf{a}_m \right)^* \left( y_{d+m+M} \mathbf{a}_m \right) \\ &= \frac{1}{M} \sum_{m=0}^{M-1} \left( |r_m|^2 |\mathbf{a}_m|^2 + r_m w_{2,m}^* |\mathbf{a}_m|^2 + r_m^* w_{1,m} |\mathbf{a}_m|^2 + w_{1,m} w_{2,m}^* |\mathbf{a}_m|^2 \right). \end{aligned} \quad (4.39)$$

From the central limit theorem, the random variable  $T$  has an asymptotic complex gaussian distribution. The mean value of  $T$ , for  $0 \leq d < L$ , is given by <sup>2</sup>

$$E[T(d)] = \sigma_a^4 \quad (4.40)$$

and the variance

$$\begin{aligned} \text{var}(T) &= E \left[ \left| T - E(T) \right|^2 \right] \\ &= \frac{1}{M} \left( 5\sigma_a^8 + 4\sigma_a^6 \sigma_w^2 + 2\sigma_a^4 \sigma_w^4 \right). \end{aligned} \quad (4.41)$$

Having computed the mean value and the variance of the complex gaussian random variable, we conclude that <sup>3</sup>  $T(d) \sim \mathcal{CN} \left( \sigma_a^4, \frac{1}{M} (5\sigma_a^8 + 4\sigma_a^6 \sigma_w^2 + 2\sigma_a^4 \sigma_w^4) \right)$ , for  $0 \leq d < L$ .

---

<sup>2</sup>See Appendix 4B for the analytical computation of the mean and the variance.

<sup>3</sup>The real and imaginary part of  $T$  is Gaussian distributed with the half variance of  $T$  (Appendix 4C).

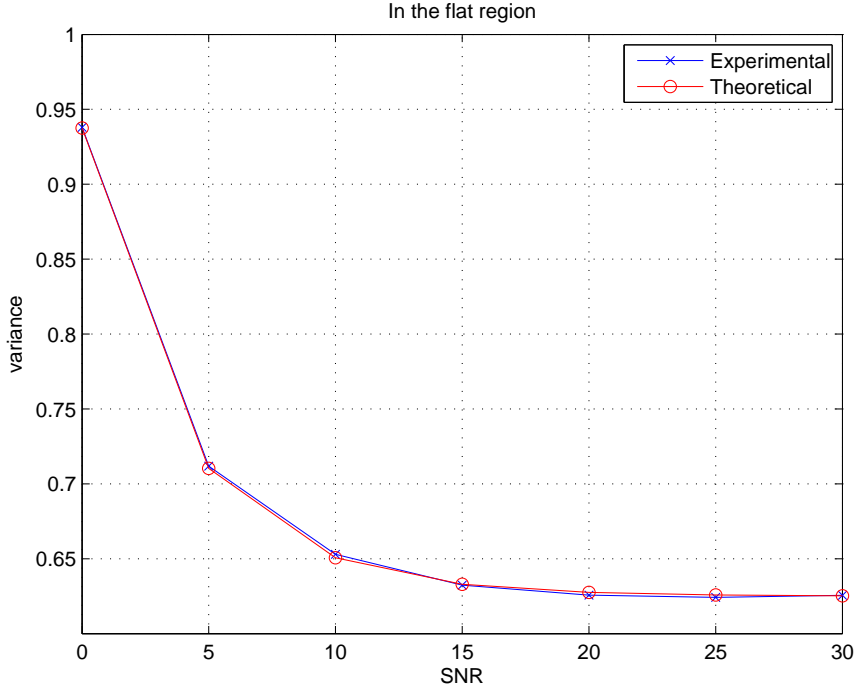


Figure 4.13: Variance of  $T$ .

Now, we analyze the case that  $d$  corresponds to the correct timing  $d_*$ . Then,

$$a_m = s_{d_*+m} = s_{d_*+m+M}, \quad (4.42)$$

and for simplicity, by defining

$$w_{1,m} := w_{d_*+m}, \quad w_{2,m} := w_{d_*+m+M}, \quad (4.43)$$

we get

$$\begin{aligned} T(d_*) &= \frac{1}{M} \sum_{m=0}^{M-1} \left( y_{d_*+m} a_m \right)^* \left( y_{d_*+m+M} a_m \right) \\ &= \frac{1}{M} \sum_{m=0}^{M-1} \left( |a_m|^4 + a_m w_{2,m}^* |a_m|^2 + a_m^* w_{1,m} |a_m|^2 + w_{1,m} w_{2,m}^* |a_m|^2 \right). \end{aligned} \quad (4.44)$$

The mean value of the complex gaussian random variable  $T$ , for  $d = d_*$ , is given by <sup>4</sup>

$$E[T(d_*)] = 2\sigma_a^4 \quad (4.45)$$

and the variance

$$\begin{aligned} \text{var}(T(d_*)) &= E \left[ \left| T - E(T) \right|^2 \right] \\ &= \frac{1}{M} (20\sigma_a^8 + 12\sigma_a^6\sigma_w^2 + 2\sigma_a^4\sigma_w^4). \end{aligned} \quad (4.46)$$

Having computed the mean value and the variance of the complex gaussian random variable, at the correct timing  $d_*$ , we conclude that  $T(d_*) \sim \mathcal{CN} \left( 2\sigma_a^4, \frac{1}{M} (20\sigma_a^8 + 12\sigma_a^6\sigma_w^2 + 2\sigma_a^4\sigma_w^4) \right)$ .

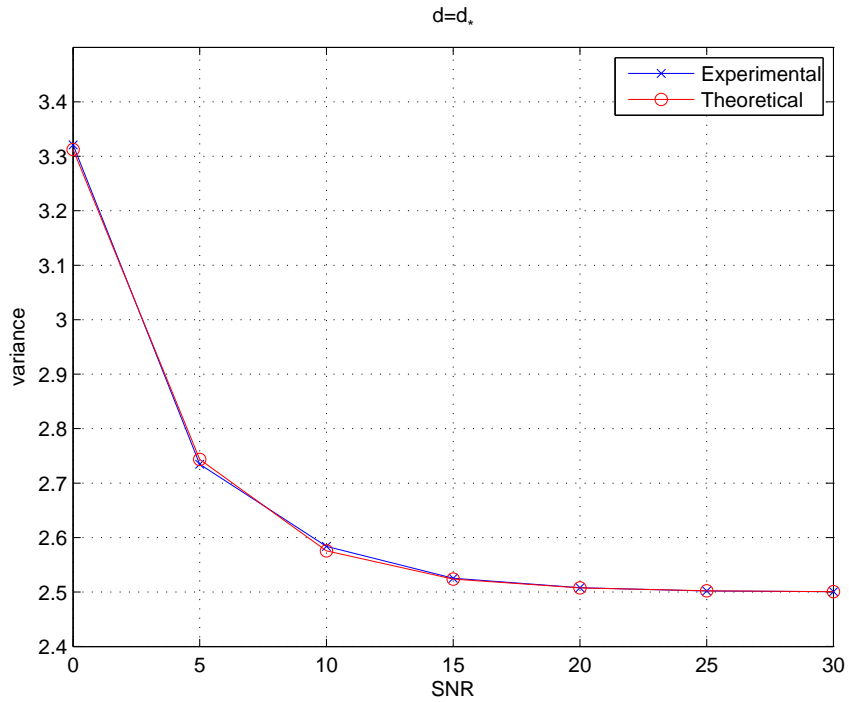


Figure 4.14: Variance of  $T(d_*)$ .

<sup>4</sup>See Appendix 4B for the analytical computation of the mean and the variance.

#### 4.1.4 Probability of correct symbol timing synchronization

In this section we assume that the receiver has detected a correct packet for processing. In order to evaluate the probability of the correct symbol timing synchronization, we will deal with the real part of the random variable  $T(d)$ . In the previous section, we have computed that

$$T(d) \sim \mathcal{CN} \left( \sigma_a^4, \frac{1}{M} (5\sigma_a^8 + 4\sigma_a^6\sigma_w^2 + 2\sigma_a^4\sigma_w^4) \right), \text{ for } 0 \leq d < L$$

and

$$T(d_*) \sim \mathcal{CN} \left( 2\sigma_a^4, \frac{1}{M} (20\sigma_a^8 + 12\sigma_a^6\sigma_w^2 + 2\sigma_a^4\sigma_w^4) \right), \text{ for } d = d_*.$$

The real part of the complex gaussian random variable  $T(d)$  is gaussian distributed with the same mean value but with the half variance<sup>5</sup> of the variable  $T(d)$ . Thus,

$$\mathcal{R}\{T(d)\} \sim \mathcal{N} \left( \sigma_a^4, \frac{1}{2M} (5\sigma_a^8 + 4\sigma_a^6\sigma_w^2 + 2\sigma_a^4\sigma_w^4) \right), \text{ for } 0 \leq d < L$$

and

$$\mathcal{R}\{T(d_*)\} \sim \mathcal{N} \left( 2\sigma_a^4, \frac{1}{2M} (20\sigma_a^8 + 12\sigma_a^6\sigma_w^2 + 2\sigma_a^4\sigma_w^4) \right), \text{ for } d = d_*.$$

We view the problem of the correct symbol timing synchronization as an attempt to distinguish if the value of  $\mathcal{R}\{T(d_*)\}$  exceeds a threshold and also is greater than all the other values of  $\mathcal{R}\{T(d)\}$ , for  $0 \leq d < L$ . If this is satisfied, we declare the detection as correct symbol timing. If  $\mathcal{R}\{T(d_*)\}$  is less than the value of the threshold or less than at least one value of  $\mathcal{R}\{T(d)\}$  for  $d \neq d_*$ , we declare an incorrect symbol timing synchronization.

Thus, the probability of finding the correct time index is defined as

---

<sup>5</sup>See Appendix 4D.

$$P_c(\tau) = P\left(\mathcal{R}\{T(d = d_*)\} > \mathcal{R}\{T(d = 0)\} \cap \mathcal{R}\{T(d = d_*)\} > \mathcal{R}\{T(d = 1)\} \cap \dots \right. \\ \left. \cap \mathcal{R}\{T(d = d_*)\} > \mathcal{R}\{T(d = L - 1)\} \cap \mathcal{R}\{T(d = d_*)\} > \tau\right), \quad (4.47)$$

where  $\tau$  is the threshold. For different values of the time index  $d$ , the values of the random variable  $\mathcal{R}\{T(d)\}$  are asymptotically, for large  $M$ , independent <sup>6</sup>. Consequently,

$$P_c(\tau) = \int_{\tau}^{\infty} f_{\mathcal{R}\{T(d_*)\}}(x) P\left(x > \mathcal{R}\{T(d = 0)\} \cap \dots \cap x > \mathcal{R}\{T(d = L - 1)\} \mid \mathcal{R}\{T(d_*)\} = x\right) dx \\ = \int_{\tau}^{\infty} f_{\mathcal{R}\{T(d_*)\}}(x) \left[ \prod_{i=0}^{L-1} P(\mathcal{R}\{T(d = i)\} < x) \right] dx \\ = \int_{\tau}^{\infty} f_{\mathcal{R}\{T(d_*)\}}(x) \left[ \prod_{i=0}^{L-1} \left(1 - Q\left(\frac{x - \mu_1}{\sigma_1}\right)\right) \right] dx \\ = \int_{\tau}^{\infty} f_{\mathcal{R}\{T(d_*)\}}(x) \left[ \left(1 - Q\left(\frac{x - \mu_1}{\sigma_1}\right)\right)^{L-1} \right] dx, \quad (4.48)$$

where  $\mu_1$  and  $\sigma_1^2$  is the mean value and the variance of  $\mathcal{R}\{T(d)\}$ , for  $0 \leq d < L$ .

We computed the probabilities of correct detections for different values of the threshold using the equation 4.48 and we verified the results with simulation experiments. The results are shown in Figure 4.15 and we observe that the simulation results are the same with those predicted by theory. The modulation used in the experiments was 4-QAM. This means that  $E(\mathcal{R}\{T(d)\}) = \sigma_x^4 = 4$ , for  $0 \leq d < L$  and  $E(\mathcal{R}\{T(d_*)\}) = 2\sigma_x^4 = 8$  for  $d = d_*$ . If the threshold is set too high, we observe that the probability of correct detection is decreased. This happens for  $\tau > 7$  because the maximum value of  $\mathcal{R}\{T(d)\}$  may not exceed this threshold, which results to an incorrect detection.

For  $\tau < 7$  the detection is correct with very high probability because the value of  $\mathcal{R}\{T(d)\}$  at the correct time index almost always exceeds the threshold and is greater than

---

<sup>6</sup>See Appendix 4D for the proof.

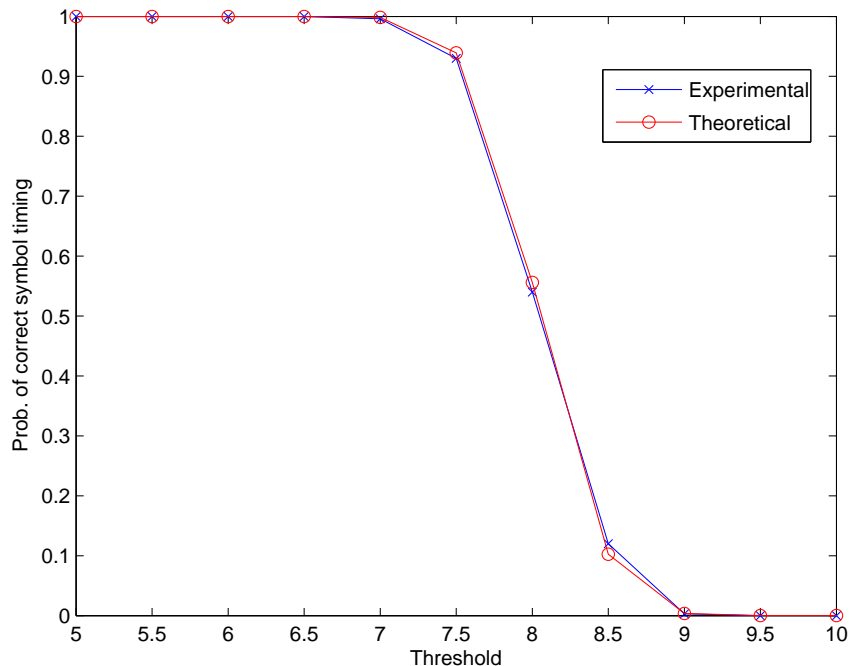


Figure 4.15: Probability of correct symbol timing, SNR = 10db.

all the other values of  $\mathcal{R}\{T(d)\}$ . This happens because we have assumed that we processed a correct packet. In the case of a false packet detection, we could not use a low threshold ( $\tau < 7$ ) because this will lead us to an incorrect symbol timing synchronization. Thus, it is desirable to use a threshold close to the mean value of  $\mathcal{R}\{T(d_*)\}$ , in order to avoid errors from the packet detection processing.

In Figure 4.16, we fixed the value of the threshold and we compute the probability of correct symbol timing for different values of SNR. For  $\tau = 7$  and SNR  $> 0$ , we observe that the symbol timing synchronization is almost always correct. If we increase the threshold ( $\tau = 7.5$ ) the probability of correct symbol timing is decreased because there are cases where the timing metric does not exceed the threshold.

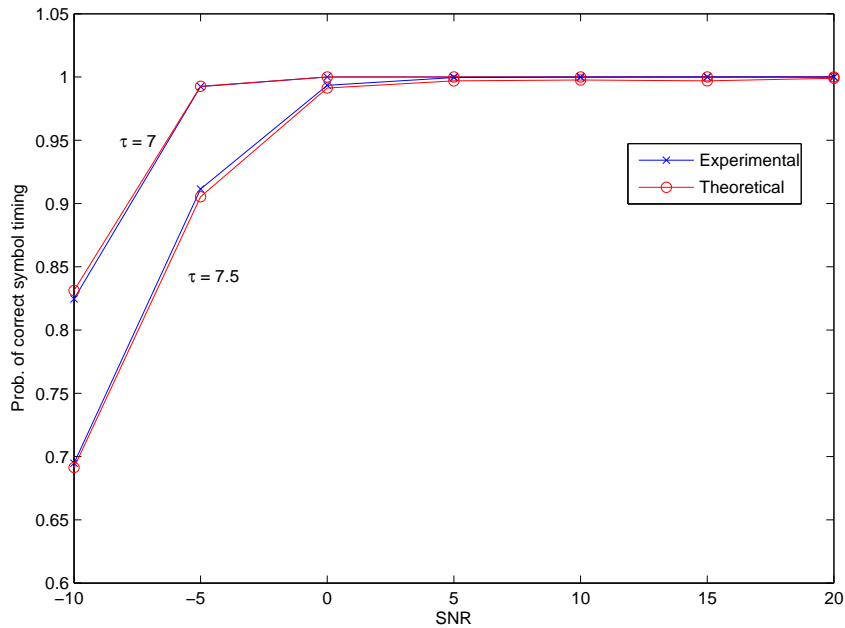


Figure 4.16: Probability of correct symbol timing vs SNR

## 4.2 Carrier Frequency Offset Synchronization

In OFDM, the uncertainty in carrier frequency, which is due to a difference in the frequencies of the local oscillators in the transmitter and receiver, causes a shift in the frequency domain. This shift is also referred to as *carrier frequency offset*. The demodulation of a signal with an offset in the carrier frequency can cause large bit error rate. It is therefore important to estimate the carrier frequency offset and eliminate its impact.

The carrier frequency offset is estimated after time synchronization. Assuming that time synchronization has already been achieved, so the receiver has identified the start of the received OFDM block, the received signal due to carrier frequency offset can be expressed as

$$y_n = e^{\frac{j2\pi\epsilon n}{N}} \sum_{l=0}^{L-1} h_l x_{n-l} + w_n. \quad (4.49)$$

Denoting

$$r_n = \sum_{l=0}^{L-1} h_l x_{n-l}, \quad (4.50)$$

then, the received samples can be expressed as

$$y_n = e^{\frac{j2\pi\epsilon n}{N}} r_n + w_n. \quad (4.51)$$

In order to estimate the carrier frequency offset, the receiver exploits the special structure of the OFDM synchronization symbol, which was also used for time synchronization. As we have mentioned, in this pilot symbol, the second half is equal to the first half. It is important to note that the main difference between the two halves of the pilot symbol will be a phase shift. If the received samples corresponding to the first half are given by

$$y_n = e^{\frac{j2\pi\epsilon n}{N}} r_n + w_n, \quad (4.52)$$

then the samples in the second half take the form

$$y_{n+\frac{N}{2}} = e^{\frac{j2\pi\epsilon\left(n+\frac{N}{2}\right)}{N}} r_{n+\frac{N}{2}} + w_{n+\frac{N}{2}} \quad (4.53)$$

$$= e^{\frac{j2\pi\epsilon\left(n+\frac{N}{2}\right)}{N}} r_n + w_{n+\frac{N}{2}}, \quad (4.54)$$

where has been used that  $r_n$  and  $r_{n+\frac{N}{2}}$  are identical.

Consequently,

$$\begin{aligned} y_n^* y_{n+\frac{N}{2}} &= \left( e^{\frac{j2\pi\epsilon n}{N}} r_n + w_n \right)^* \left( e^{\frac{j2\pi\epsilon\left(n+\frac{N}{2}\right)}{N}} r_n + w_{n+\frac{N}{2}} \right) \quad (4.55) \\ &= e^{-\frac{j2\pi\epsilon n}{N}} r_n^* e^{\frac{j2\pi\epsilon\left(n+\frac{N}{2}\right)}{N}} r_n + e^{-\frac{j2\pi\epsilon n}{N}} r_n^* w_{n+\frac{N}{2}} + w_n^* e^{\frac{j2\pi\epsilon\left(n+\frac{N}{2}\right)}{N}} r_n + w_n^* w_{n+\frac{N}{2}} \\ &= e^{j\pi\epsilon} |r_n|^2 + \tilde{w}_n, \end{aligned}$$

where

$$\tilde{w}_n = e^{-\frac{j2\pi\epsilon n}{N}} r_n^* w_{n+\frac{N}{2}} + w_n^* e^{\frac{j2\pi\epsilon(n+\frac{N}{2})}{N}} r_n + w_n^* w_{n+\frac{N}{2}}. \quad (4.56)$$

Ignoring the noise part, if we take the argument of  $y_n^* y_{n+\frac{N}{2}}$ , then an estimate of  $\epsilon$  can be derived. Using all the samples of the pilot symbol, the carrier frequency offset can be estimated by

$$\hat{\epsilon} = \frac{1}{\pi} \arg \left( \sum_{n=0}^{\frac{N}{2}-1} y_n^* y_{n+\frac{N}{2}} \right), \quad (4.57)$$

because

$$\arg \left( \sum_{n=0}^{\frac{N}{2}-1} y_n y_{n+\frac{N}{2}}^* \right) = \arg \left( e^{j\pi\epsilon} \sum_{n=0}^{\frac{N}{2}-1} |r_n|^2 \right) = \pi\epsilon.$$

## Appendix 4A: Moments of a zero-mean complex scalar-valued random variable

For the computation of the moments of a zero-mean complex scalar-valued random variable, we have used the moments of a Gaussian random variable.

$$\text{If } x \sim \mathcal{N}(0, \sigma^2) \text{ then } E[x^n] = \begin{cases} 1 \cdot 3 \cdot 5 \cdots (n-1)\sigma^n, & n \text{ even} \\ 0, & n \text{ odd.} \end{cases}$$

The **fourth-order moment** of a zero-mean complex scalar-valued random variable  $a$ , is given by

$$\begin{aligned} E[|a|^4] &= E[|a_R + ja_I|^4] = E[|a_R + ja_I|^2 |a_R + ja_I|^2] & (4.58) \\ &= E[(a_R + ja_I)(a_R + ja_I)^*(a_R + ja_I)(a_R + ja_I)^*] \\ &= E[(a_R + ja_I)(a_R - ja_I)(a_R + ja_I)(a_R - ja_I)] \\ &= E[(a_R^2 - ja_R a_I + ja_R a_I + a_I^2)(a_R^2 + a_I^2)] \\ &= E[a_R^4 + 2a_R^2 a_I^2 + a_I^4] = E[a_R^4] + 2E[a_R^2]E[a_I^2] + E[a_I^4] \\ &= 3\left(\frac{\sigma_a^2}{2}\right)^2 + 2\frac{\sigma_a^2}{2}\frac{\sigma_a^2}{2} + 3\left(\frac{\sigma_a^2}{2}\right)^2 = 2\sigma_a^4. \end{aligned}$$

where  $a_R$  and  $a_I$  is the real and imaginary part of the complex random variable  $a$ , respectively.  $a_R$  and  $a_I$  are independent zero-mean gaussian random variables with variance  $\frac{\sigma_a^2}{2}$ .

The **sixth-order moment** of a zero-mean complex scalar-valued random variable  $a$ ,

is given by

$$\begin{aligned}
E[|a|^6] &= E[|a_R + ja_I|^6] = E[|a_R + ja_I|^2 |a_R + ja_I|^2 |a_R + ja_I|^2] \\
&= E[(a_R^2 + a_I^2)(a_R^2 + a_I^2)(a_R^2 + a_I^2)] = E[(a_R^4 + 2a_R^2 a_I^2 + a_I^4)(a_R^2 + a_I^2)] \\
&= E[a_R^6 + 3a_R^4 a_I^2 + 3a_I^4 a_R^2 + a_I^6] = 2E[a_R^6] + 3E[a_R^4 a_I^2] + 3E[a_I^4 a_R^2] \\
&= 2 \cdot 3 \cdot 5 \left(\frac{\sigma_a^2}{2}\right)^3 + 2 \cdot 3 \cdot 3 \left(\frac{\sigma_a^2}{2}\right)^2 \frac{\sigma_a^2}{2} = 6\sigma_a^6,
\end{aligned} \tag{4.59}$$

The **eighth-order moment** of a zero-mean complex scalar-valued random variable  $a$ , is given by

$$\begin{aligned}
E[|a|^8] &= E[|a_R + ja_I|^8] \\
&= E[|a_R + ja_I|^2 |a_R + ja_I|^2 |a_R + ja_I|^2 |a_R + ja_I|^2] \\
&= E[(a_R^2 + a_I^2)(a_R^2 + a_I^2)(a_R^2 + a_I^2)(a_R^2 + a_I^2)] \\
&= 2E[a_R^8] + 4E[a_R^6 a_I^2] + 6E[a_R^4 a_I^4] + 4E[a_R^2 a_I^6] \\
&= 24\sigma_a^8.
\end{aligned} \tag{4.60}$$

## Appendix 4B: Computation of the mean and variance of the pilot based metric

Assuming that  $d$  corresponds to a sample in the interval of the cyclic prefix,  $0 \leq d < L$ , we compute the mean value of the metric

$$E[T(d)] = \frac{1}{M} \sum_{m=0}^{M-1} E[|r_m|^2 |a_m|^2] + \underbrace{\frac{1}{M} \sum_{m=0}^{M-1} E[r_m w_{2,m}^* |a_m|^2 + r_m^* w_{1,m} |a_m|^2 + w_{1,m} w_{2,m}^* |a_m|^2]}_{\mathcal{A}_1} \tag{4.61}$$

$$\stackrel{r,a \text{ ind.}}{=} \frac{1}{M} \sum_{m=0}^{M-1} E[|r_m|^2] E[|a_m|^2] + \mathcal{A}_1 = \sigma_r^2 \sigma_a^2 + \mathcal{A}_1,$$

where

$$\begin{aligned}
\mathcal{A}_1 &= \frac{1}{M} \sum_{m=0}^{M-1} E \left[ r_m w_{2,m}^* |a_m|^2 + r_m^* w_{1,m} |a_m|^2 + w_{1,m} w_{2,m}^* |a_m|^2 \right] \\
&= \frac{1}{M} \sum_{m=0}^{M-1} \left\{ E[r_m] E[w_{2,m}^*] E[|a_m|^2] + E[r_m^*] E[w_{1,m}] E[|a_m|^2] + E[w_{1,m}] E[w_{2,m}^*] E[|a_m|^2] \right\} \\
&= 0.
\end{aligned} \tag{4.62}$$

The variables  $r_m$  and  $a_m$  have the same distribution,  $\mathcal{CN}(0, \sigma_a^2)$ , thus,

$$E[T(d)] = \sigma_a^4, \text{ for } 0 \leq d < L. \tag{4.63}$$

Without loss of generality, dropping the time index  $d$ , the variance of the random variable  $T$  is

$$\text{var}(T) = E \left[ \left| T - E(T) \right|^2 \right]. \tag{4.64}$$

If we define

$$\mathcal{B}_m = |r_m|^2 |a_m|^2 + r_m w_{2,m}^* |a_m|^2 + r_m^* w_{1,m} |a_m|^2 + w_{1,m} w_{2,m}^* |a_m|^2, \tag{4.65}$$

and drop the subscript  $m$ , we obtain

$$\begin{aligned}
E[\mathcal{B}] &= E \left[ |r|^2 |a|^2 + r w_2^* |a|^2 + r^* w_1 |a|^2 + w_1 w_2^* |a|^2 \right] \\
&= \sigma_r^2 \sigma_a^2 = \sigma_a^4,
\end{aligned} \tag{4.66}$$

and

$$\begin{aligned}
E[\mathcal{B}\mathcal{B}^*] &= E\left[\left(|r|^2|a|^2 + rw_2^*|a|^2 + r^*w_1|a|^2 + w_1w_2^*|a|^2\right)\right. \\
&\quad \left. \left(|r|^2|a|^2 + r^*w_2|a|^2 + rw_1^*|a|^2 + w_1^*w_2|a|^2\right)\right] \\
&= E\left[|r|^4|a|^4\right] + E\left[|r|^2|w_2|^2|a|^4\right] + E\left[|r|^2|w_1|^2|a|^4\right] + E\left[|w_1|^2|w_2|^2|a|^4\right] \\
&= 4\sigma_a^8 + 4\sigma_a^6\sigma_w^2 + 2\sigma_w^4\sigma_a^4.
\end{aligned} \tag{4.67}$$

Using equations (4.66) and (4.67), we get

$$\begin{aligned}
\text{var}(T) &= E\left[|T - E(T)|^2\right] = E\left[\left|\left(\frac{1}{M}\sum_{m=0}^{M-1}\mathcal{B}_m\right) - \sigma_a^4\right|^2\right] \\
&= E\left[\left|\frac{1}{M}\sum_{m=0}^{M-1}(\mathcal{B}_m - \sigma_a^4)\right|^2\right] = \frac{1}{M^2}\sum_{m=0}^{M-1}\sum_{k=0}^{M-1}E\left[(\mathcal{B}_m - \sigma_a^4)(\mathcal{B}_k - \sigma_a^4)^*\right] \\
&= \underbrace{\frac{1}{M^2}\sum_{m=0}^{M-1}E\left[|\mathcal{B}_m - \sigma_a^4|^2\right]}_{\mathcal{C}_1} + \underbrace{\frac{1}{M^2}\sum_{m=0}^{M-1}\sum_{\substack{k=0 \\ k \neq m}}^{M-1}E\left[(\mathcal{B}_m - \sigma_a^4)(\mathcal{B}_k - \sigma_a^4)^*\right]}_{\mathcal{D}_1},
\end{aligned} \tag{4.68}$$

$$\tag{4.69}$$

where

$$\begin{aligned}
\mathcal{C}_1 &= \frac{1}{M^2}\sum_{m=0}^{M-1}E\left[|\mathcal{B}_m - \sigma_a^4|^2\right] = \frac{1}{M}E\left[|\mathcal{B} - \sigma_a^4|^2\right] \\
&= \frac{1}{M}E\left[(\mathcal{B} - \sigma_a^4)(\mathcal{B} - \sigma_a^4)^*\right] = \frac{1}{M}E\left[\mathcal{B}\mathcal{B}^* - \mathcal{B}\sigma_a^4 - \mathcal{B}^*\sigma_a^4 + \sigma_a^8\right] \\
&= \frac{1}{M}\left(E\left[\mathcal{B}\mathcal{B}^*\right] - 2\sigma_a^4E\left[\mathcal{B}\right] + \sigma_a^8\right) \stackrel{\sigma_r^2 = \sigma_a^2}{=} \frac{1}{M}\left(3\sigma_a^8 + 4\sigma_a^6\sigma_w^2 + 2\sigma_a^4\sigma_w^4\right),
\end{aligned} \tag{4.70}$$

and

$$\mathcal{D}_1 = \frac{1}{M^2} \sum_{m=0}^{M-1} \sum_{\substack{k=0 \\ k \neq m}}^{M-1} E [(\mathcal{B}_m - \sigma_a^4) (\mathcal{B}_k - \sigma_a^4)^*] \quad (4.71)$$

$$\begin{aligned} &= \frac{1}{M^2} \left\{ (M^2 - M - 2M) E [2|r_m|^2 |a_m|^2 |r_k|^2 |a_k|^2 - 2|r_m|^2 |a_m|^2 \sigma_a^4] \right. \\ &\quad \left. + 2M (E [|r_m|^4 |a_m|^2 |a_k|^2 - |r_m|^2 |a_m|^2 \sigma_a^4]) \right\} \\ &= \frac{2}{M} \sigma_a^8. \end{aligned} \quad (4.72)$$

Thus, substituting equations (4.70) and (4.72) in (4.69), we get

$$\begin{aligned} \text{var}(T) &= \mathcal{C}_1 + \mathcal{D}_1 \\ &= \frac{1}{M} (5\sigma_a^8 + 4\sigma_a^6 \sigma_w^2 + 2\sigma_a^4 \sigma_w^4). \end{aligned} \quad (4.73)$$

We conclude that

$$T(d) \sim \mathcal{CN} \left( \sigma_a^4, \frac{1}{M} (5\sigma_a^8 + 4\sigma_a^6 \sigma_w^2 + 2\sigma_a^4 \sigma_w^4) \right), \text{ for } 0 \leq d < L. \quad (4.74)$$

Now, we analyze the case where  $d$  corresponds to the correct timing  $d_*$ . Computing the mean value

$$E[T(d_*)] = \frac{1}{M} \sum_{m=0}^{M-1} E[|a_m|^4] + \underbrace{\frac{1}{M} \sum_{m=0}^{M-1} E[a_m w_{2,m}^* |a_m|^2 + a_m^* w_{1,m} |a_m|^2 + w_{1,m} w_{2,m}^* |a_m|^2]}_{\mathcal{A}_2} \quad (4.75)$$

$$\stackrel{\mathcal{A}_2=0}{=} \frac{1}{M} \sum_{m=0}^{M-1} E[|a_m|^4] = E[|a|^4] \stackrel{(4.58)}{=} 2\sigma_a^4.$$

Dropping the time index  $d_*$ , the variance of the random variable  $T$  is

$$\text{var}(T) = E [|T - E(T)|^2]. \quad (4.76)$$

We define

$$\mathcal{R}_m = |a_m|^4 + a_m w_{2,m}^* |a_m|^2 + a_m^* w_{1,m} |a_m|^2 + w_{1,m} w_{2,m}^* |a_m|^2, \quad (4.77)$$

Using the following results

$$E[\mathcal{R}] = E [|a|^4 + a w_2^* |a|^2 + a^* w_1 |a|^2 + w_1 w_2^* |a|^2] \stackrel{(4.58)}{=} 2\sigma_a^4, \quad (4.78)$$

and

$$\begin{aligned} E[\mathcal{R}\mathcal{R}^*] &= E [ (|a|^4 + a w_2^* |a|^2 + a^* w_1 |a|^2 + w_1 w_2^* |a|^2) (|a|^4 + a^* w_2 |a|^2 + a w_1^* |a|^2 + w_1^* w_2 |a|^2) ] \\ &= E [|a|^8] + E [|w_2|^2 |a|^6] + E [|w_1|^2 |a|^6] + E [|w_1|^2 |w_2|^2 |a|^4] \\ &\stackrel{(4.59), (4.60)}{=} 24\sigma_a^8 + 12\sigma_a^6 \sigma_w^2 + 2\sigma_w^4 \sigma_a^4, \end{aligned}$$

we get

$$\begin{aligned} \text{var}(T) &= E \left[ |T - E(T)|^2 \right] = E \left[ \left| \left( \frac{1}{M} \sum_{m=0}^{M-1} \mathcal{R}_m \right) - 2\sigma_a^4 \right|^2 \right] \\ &= E \left[ \left| \frac{1}{M} \sum_{m=0}^{M-1} (\mathcal{R}_m - 2\sigma_a^4) \right|^2 \right] = \frac{1}{M^2} \sum_{m=0}^{M-1} \sum_{k=0}^{M-1} E [ (\mathcal{R}_m - 2\sigma_a^4) (\mathcal{R}_k - 2\sigma_a^4)^* ] \\ &= \underbrace{\frac{1}{M^2} \sum_{m=0}^{M-1} E [ |\mathcal{R}_m - 2\sigma_a^4|^2 ]}_{\mathcal{C}_2} + \underbrace{\frac{1}{M^2} \sum_{m=0}^{M-1} \sum_{\substack{k=0 \\ k \neq m}}^{M-1} E [ (\mathcal{R}_m - 2\sigma_a^4) (\mathcal{R}_k - 2\sigma_a^4)^* ]}_{\mathcal{D}_2}, \quad (4.79) \end{aligned}$$

where

$$\begin{aligned}
\mathcal{C}_2 &= \frac{1}{M^2} \sum_{m=0}^{M-1} E \left[ |\mathcal{R}_m - 2\sigma_a^4|^2 \right] = \frac{1}{M} E \left[ |\mathcal{R} - 2\sigma_a^4|^2 \right] \\
&= \frac{1}{M} E \left[ (\mathcal{R} - 2\sigma_a^4) (\mathcal{R} - 2\sigma_a^4)^* \right] = \frac{1}{M} E \left[ \mathcal{R}\mathcal{R}^* - \mathcal{R}2\sigma_a^4 - \mathcal{R}^*2\sigma_a^4 + 4\sigma_a^8 \right] \\
&= \frac{1}{M} \left( E \left[ \mathcal{R}\mathcal{R}^* \right] - 4\sigma_a^4 E \left[ \mathcal{R} \right] + \sigma_a^8 \right) = \frac{1}{M} \left( 20\sigma_a^8 + 12\sigma_a^6\sigma_w^2 + 2\sigma_a^4\sigma_w^4 \right),
\end{aligned} \tag{4.80}$$

and

$$\begin{aligned}
\mathcal{D}_2 &= \frac{1}{M^2} \sum_{m=0}^{M-1} \sum_{\substack{k=0 \\ k \neq m}}^{M-1} E \left[ \mathcal{R}_m - 2\sigma_a^4 \right] \left[ \mathcal{R}_k - 2\sigma_a^4 \right]^* \\
&= \frac{1}{M^2} (M^2 - M) E \left[ |a_m|^4 |a_k|^4 - 4|a_m|^4 \sigma_a^4 + 4\sigma_a^4 \sigma_a^4 \right] = 0.
\end{aligned} \tag{4.81}$$

Thus, substituting equations (4.80) and (4.81) in (4.79) we get

$$\begin{aligned}
\text{var}(T) &= \mathcal{C}_2 + \mathcal{D}_2 \\
&= \frac{1}{M} \left( 20\sigma_a^8 + 12\sigma_a^6\sigma_w^2 + 2\sigma_a^4\sigma_w^4 \right).
\end{aligned} \tag{4.82}$$

We conclude that

$$T(d_*) \sim \mathcal{CN} \left( 2\sigma_a^4, \frac{1}{M} \left( 20\sigma_a^8 + 12\sigma_a^6\sigma_w^2 + 2\sigma_a^4\sigma_w^4 \right) \right). \tag{4.83}$$

## Appendix 4C: Variance equality of the real and imaginary part of the pilot based metric

We will prove that the real part of the complex gaussian random variable  $T$  has the same distribution with the imaginary part of  $T$  with variance the half of the variable  $T$ . The random variable  $T$  is defined as

$$T = \frac{1}{M} \sum_{m=0}^{M-1} \left( |r_m|^2 |a_m|^2 + r_m w_{2,m}^* |a_m|^2 + r_m^* w_{1,m} |a_m|^2 + w_{1,m} w_{2,m}^* |a_m|^2 \right).$$

We drop the subscript  $m$  and define the complex gaussian random variable

$$\mathcal{D} = rw_2^* + r^*w_1 + w_1w_2^*. \quad (4.84)$$

We compute the mean value

$$E[\mathcal{D}] = E[rw_2^* + r^*w_1 + w_1w_2^*] = E[rw_2^*] + E[r^*w_1] + E[w_1w_2^*] = 0 \quad (4.85)$$

and the variance

$$\begin{aligned} E[\mathcal{D}\mathcal{D}^*] &= E[(rw_2^* + r^*w_1 + w_1w_2^*)(rw_2^* + r^*w_1 + w_1w_2^*)^*] \\ &= E[(rw_2^* + r^*w_1 + w_1w_2^*)(r^*w_2 + rw_1^* + w_1^*w_2)] \\ &= E[|r|^2|w_2|^2] + E[|r|^2|w_1|^2] + E[|w_1|^2|w_2|^2] \\ &= 2(\sigma_r^2\sigma_w^2) + \sigma_w^4. \end{aligned} \quad (4.86)$$

The complex gaussian random variable  $\mathcal{D}$  can also be written as

$$\begin{aligned}
\mathcal{D} &= rw_2^* + r^*w_1 + w_1w_2^* \\
&= (r_R + r_Ij)(w_{2R} + w_{2I}j)^* + (r_R + r_Ij)^*(w_{1R} + w_{1I}j) + (w_{1R} + w_{1I}j)(w_{2R} + w_{2I}j)^* \\
&= (r_R + r_Ij)(w_{2R} - w_{2I}j) + (r_R - r_Ij)(w_{1R} + w_{1I}j) + (w_{1R} + w_{1I}j)(w_{2R} - w_{2I}j) \\
&= \underbrace{(r_Rw_{2R} + r_Iw_{2I} + r_Rw_{1R} + r_Iw_{1I} + w_{1R}w_{2R} + w_{1I}w_{2I})}_{\mathcal{D}_R} \\
&\quad + \underbrace{(-r_Rw_{2I} + r_Iw_{2R} + r_Rw_{1I} - r_Iw_{1R} - w_{1R}w_{2I} + w_{1I}w_{2R})}_{\mathcal{D}_I}j.
\end{aligned}$$

The mean value of the real part ( $\mathcal{D}_R$ ) and imaginary part ( $\mathcal{D}_I$ ) is zero because of the independence of the random variables  $r$ ,  $w_1$  and  $w_2$ . The variance of the real part of  $\mathcal{D}$  is

$$\begin{aligned}
E[\mathcal{D}_R^2] &= E[(r_Rw_{2R} + r_Iw_{2I} + r_Rw_{1R} + r_Iw_{1I} + w_{1R}w_{2R} + w_{1I}w_{2I})^2] \quad (4.87) \\
&\stackrel{7}{=} E[r_R^2w_{2R}^2 + r_I^2w_{2I}^2 + r_R^2w_{1R}^2 + r_I^2w_{1I}^2 + w_{1R}^2w_{2R}^2 + w_{1I}^2w_{2I}^2] \\
&= \frac{\sigma_r^2}{2} \frac{\sigma_w^2}{2} + \frac{\sigma_r^2}{2} \frac{\sigma_w^2}{2} + \frac{\sigma_r^2}{2} \frac{\sigma_w^2}{2} + \frac{\sigma_r^2}{2} \frac{\sigma_w^2}{2} + \frac{\sigma_w^2}{2} \frac{\sigma_w^2}{2} + \frac{\sigma_w^2}{2} \frac{\sigma_w^2}{2} \\
&= \sigma_r^2 \sigma_w^2 + \frac{\sigma_w^4}{2}
\end{aligned}$$

and the variance of the imaginary part is

$$\begin{aligned}
E[\mathcal{D}_I^2] &= E[(-r_Rw_{2I} + r_Iw_{2R} + r_Rw_{1I} - r_Iw_{1R} - w_{1R}w_{2I} + w_{1I}w_{2R})^2] \quad (4.88) \\
&= E[r_R^2w_{2I}^2 + r_I^2w_{2R}^2 + r_R^2w_{1I}^2 + r_I^2w_{1R}^2 + w_{1R}^2w_{2I}^2 + w_{1I}^2w_{2R}^2] \\
&= \frac{\sigma_r^2}{2} \frac{\sigma_w^2}{2} + \frac{\sigma_r^2}{2} \frac{\sigma_w^2}{2} + \frac{\sigma_r^2}{2} \frac{\sigma_w^2}{2} + \frac{\sigma_r^2}{2} \frac{\sigma_w^2}{2} + \frac{\sigma_w^2}{2} \frac{\sigma_w^2}{2} + \frac{\sigma_w^2}{2} \frac{\sigma_w^2}{2} \\
&= \sigma_r^2 \sigma_w^2 + \frac{\sigma_w^4}{2}.
\end{aligned}$$

---

<sup>7</sup>The mean value of the products  $E[r_Rw_{2R}r_Iw_{2I}]$ ,  $\dots$ ,  $E[w_{1R}w_{2R}w_{1I}w_{2I}]$  is zero.

Thus, from equations 4.86, 4.87 and 4.88 we conclude that

$$E [\mathcal{D}_R^2] = E [\mathcal{D}_I^2] = \frac{E [\mathcal{D}\mathcal{D}^*]}{2}. \quad (4.89)$$

The same proof, but with different variances, holds for the random variable  $T$  because  $T$  is a function of  $\mathcal{D}$  and the other terms ( $|r_m|^2$  and  $|a_m|^2$ ) are real numbers.

$$T = \frac{1}{M} \sum_{m=0}^{M-1} \left[ \left( |r_m|^2 + \mathcal{D} \right) |a_m|^2 \right].$$

## Appendix 4D: Asymptotic independence of the pilot based metric for different time indices

We will prove that the pilot based metric for different values of the time index  $0 \leq d < L$  is independent. The random variable  $T$  is defined as

$$T(d) = \frac{1}{M} \sum_{m=0}^{M-1} \left( |r_{d+m}|^2 |a_m|^2 + r_{d+m} w_{2,d+m}^* |a_m|^2 + r_{d+m}^* w_{1,d+m} |a_m|^2 + w_{1,d+m} w_{2,d+m}^* |a_m|^2 \right). \quad (4.90)$$

For different values of  $d$  the mean value of  $T(d)$  is <sup>8</sup>

$$E [T(d)] = \sigma_a^4. \quad (4.91)$$

Thus, for time indices  $d_1$  and  $d_2$

$$E [T(d_1)] = E [T(d_2)] = \sigma_a^4. \quad (4.92)$$

---

<sup>8</sup>see Appendix 4B

In order to compute the quantity  $E [T(d_1)T(d_2)]$ , we keep only the term  $|r_{d+m}|^2|a_m|^2$  of equation 4.90, because the mean value of all the other products is zero (independence).

Thus, by defining

$$\mathcal{R}_{d,m} = |r_{d+m}|^2|a_m|^2, \quad (4.93)$$

we compute

$$\begin{aligned} E [T(d_1)T(d_2)] &= E \left[ \frac{1}{M} \sum_{m=0}^{M-1} (\mathcal{R}_{d_1,m}) \frac{1}{M} \sum_{k=0}^{M-1} (\mathcal{R}_{d_2,k}) \right] \\ &= \frac{1}{M^2} \sum_{m=0}^{M-1} \sum_{k=0}^{M-1} E [\mathcal{R}_{d_1,m} \mathcal{R}_{d_2,k}] \\ &= \frac{1}{M^2} \sum_{m=0}^{M-1} E [|r_{d_1+m}|^2 |r_{d_2+m}|^2 |a_m|^4] + \frac{1}{M^2} \sum_{m=0}^{M-1} \sum_{\substack{k=0 \\ k \neq m}}^{M-1} E [|r_{d_1+m}|^2 |a_m|^2 |r_{d_2+k}|^2 |a_k|^2] \\ &= \frac{1}{M} (\sigma_r^2 \sigma_r^2 2\sigma_a^4) + \frac{1}{M^2} (M^2 - M) \sigma_r^2 \sigma_r^2 \sigma_a^2 \sigma_a^2 \\ &\stackrel{\sigma_r^2 = \sigma_a^2}{=} \frac{1}{M} (2\sigma_a^8) + \sigma_a^8 - \frac{1}{M} (\sigma_a^8) = \sigma_a^8 + \frac{1}{M} \sigma_a^8. \end{aligned} \quad (4.94)$$

As we have mentioned in previous chapters, the random variable  $T$  is asymptotically complex gaussian. Thus, the second term of equation 4.94 goes to zero for large  $M$  and we get

$$E [T(d_1)T(d_2)] \simeq \sigma_a^8. \quad (4.95)$$

As a consequence,

$$E [T(d_1)T(d_2)] \simeq E [T(d_1)] E [T(d_2)] \quad (4.96)$$

which proves the independence of the variables  $T(d_1)$  and  $T(d_2)$ .

# Chapter 5

## Software-Defined Radio using USRP

### 5.1 Software-Defined Radio (SDR)

SDR is a rapidly evolving technology that is receiving enormous attention and generating widespread interest in the telecommunication industry. SDR is a revolution in radio design due to its ability to create radios that change on the fly, creating new choices for users.

An SDR system is a radio communication system which can tune to different frequency bands and use different modulations, by means of a programmable hardware which is controlled by software. The idea behind SDR is to do all the modulation and demodulation with software instead of using dedicated circuitry. Instead of having to build extra circuitry to handle different types of radio signals, we can just load an appropriate program. Based on the same hardware, different transmitter/receiver algorithms, which usually describe transmission standards, are implemented in software. By modifying or replacing software programs, we can completely change its functionality. This allows easy upgrade to new modes and improved performance without the need to replace hardware.

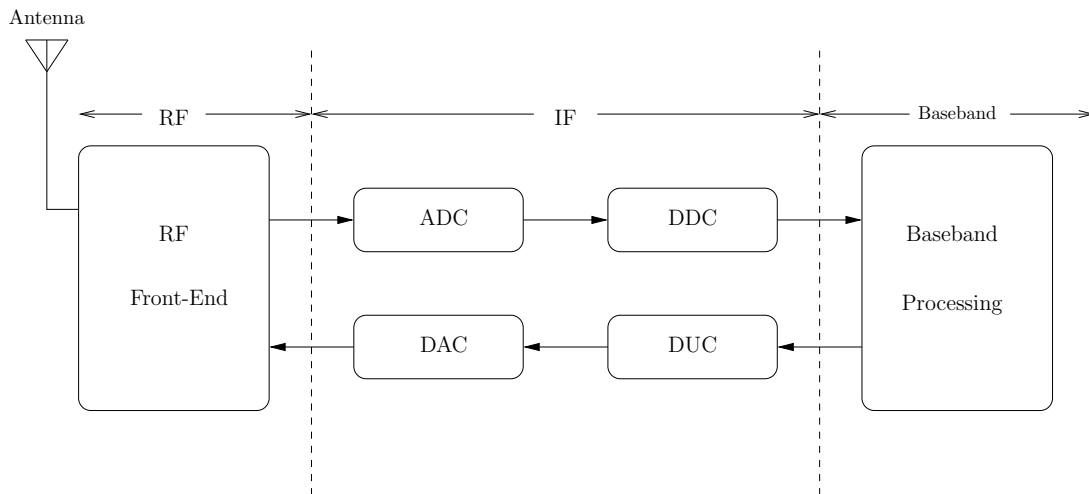


Figure 5.1: Software radio block diagram.

## 5.2 The Universal Software Radio Peripheral System (USRP)

The USRP can be used to design and implement powerful, flexible software radios. USRP is designed especially to be used with GNU Radio, which is a complete open source signal processing package, for building SDRs. The software structure of GNU Radio contains two levels. All the signal processing blocks are written in C++ and Python is used to create a network or graph and glue these blocks together.

In the USRP, high sample-rate processing takes place in the field programmable gate array (FPGA), while lower sample-rate processing happens in the host computer. FPGA takes care of decimating and interpolating of high bit rate signals in order to be transferred over the relatively slow USB link. There are 4 high-speed 12-bit A/D converters, with sampling rate 64MS/s. At the transmit path, there are also 4 high-speed 14-bit D/A converters, with sampling rate 128MS/s. On the motherboard there are four slots, where we can plug in up to 2 RX daughterboards and 2 TX daughterboards. The daughterboards mounted on the USRP provide flexible, fully integrated RF front-ends.

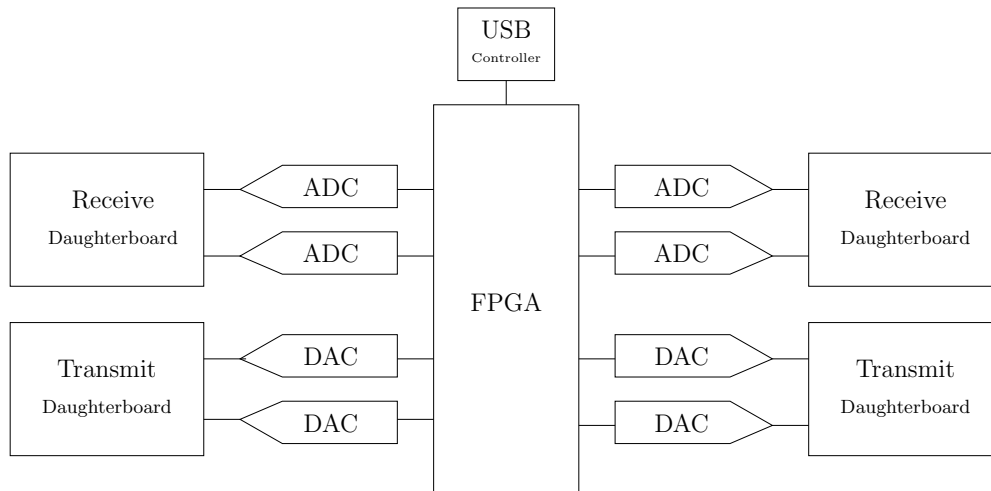


Figure 5.2: The USRP board.

### 5.3 Implementation of SDR for OFDM system - Simulations

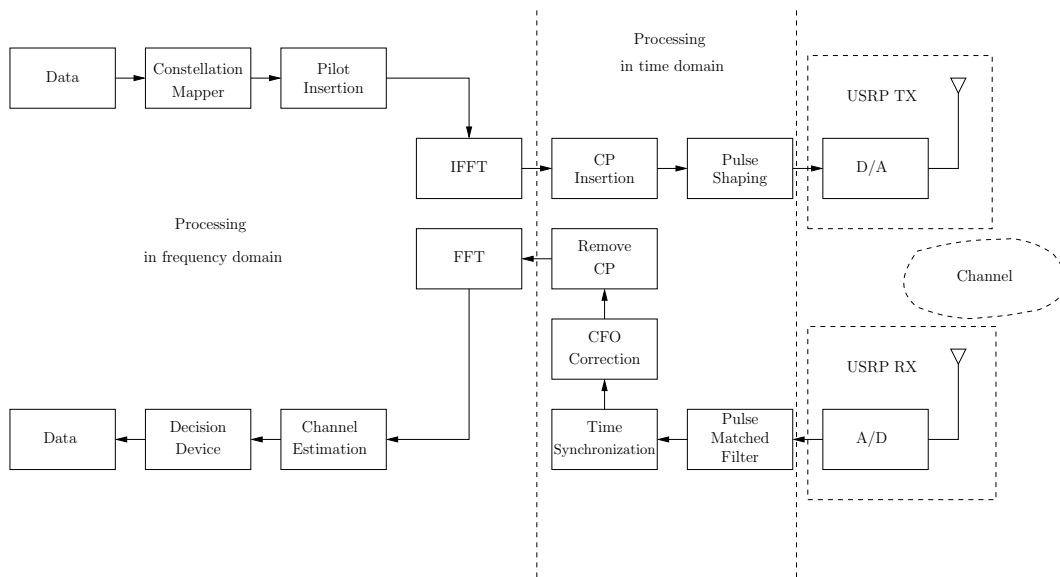


Figure 5.3: OFDM diagram.

The implementation of the OFDM system, which has been described in previous chapters, was developed and tested using USRP and GNU Radio. The modulation techniques applied were BPSK and 4-QAM. In all tests, the center frequency of the carrier wave

was adjusted to 2.5GHz. The transmission power was controlled by an amplitude gain parameter, which takes values up to 32767 and, experimentally, can be translated to dBm.

The sampling frequency of the A/D converter is 64MHz and the decimation factor sets how much decimation is done in the FPGA. Thus, the bandwidth of the signal and the bit rate is calculated by these parameters. The maximum rate can be 8MS/s, which translates to an effective bandwidth of 8MHz wide.

In our experiments, we selected the decimation factor to be 16, which means 4MHz bandwidth. Data packets consisting of random symbols with packet size of 128 symbols were sent from the transmitter to the receiver.

A packet example that receiver processes is shown in Figure 5.4. In addition, in Figure 5.5 we depict only the real part of the received signal to clearly illustrate the two successive identical pilot symbols of the preamble used for time synchronization.

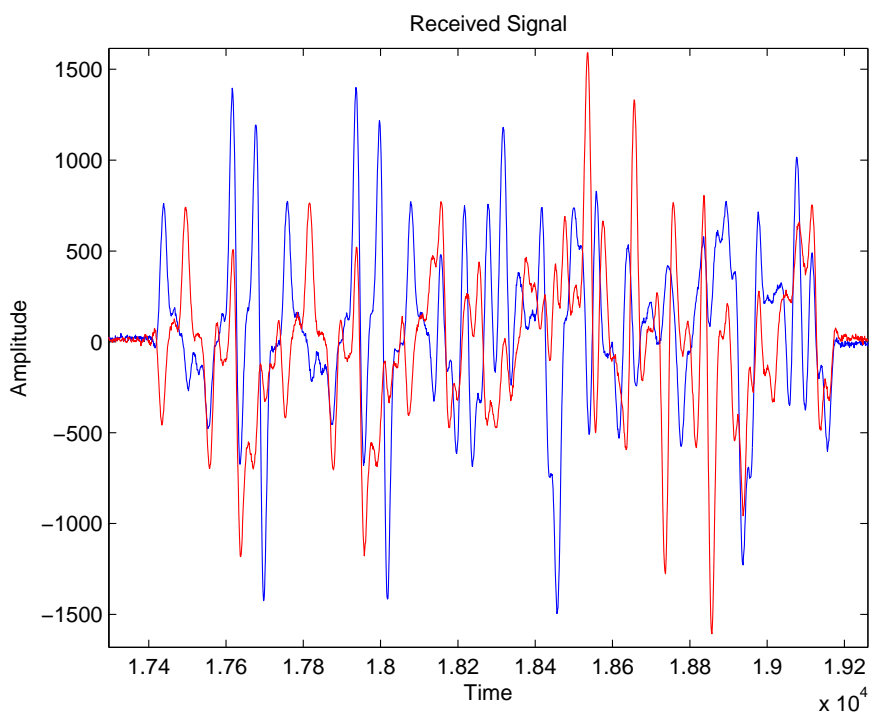


Figure 5.4: Received Signal.

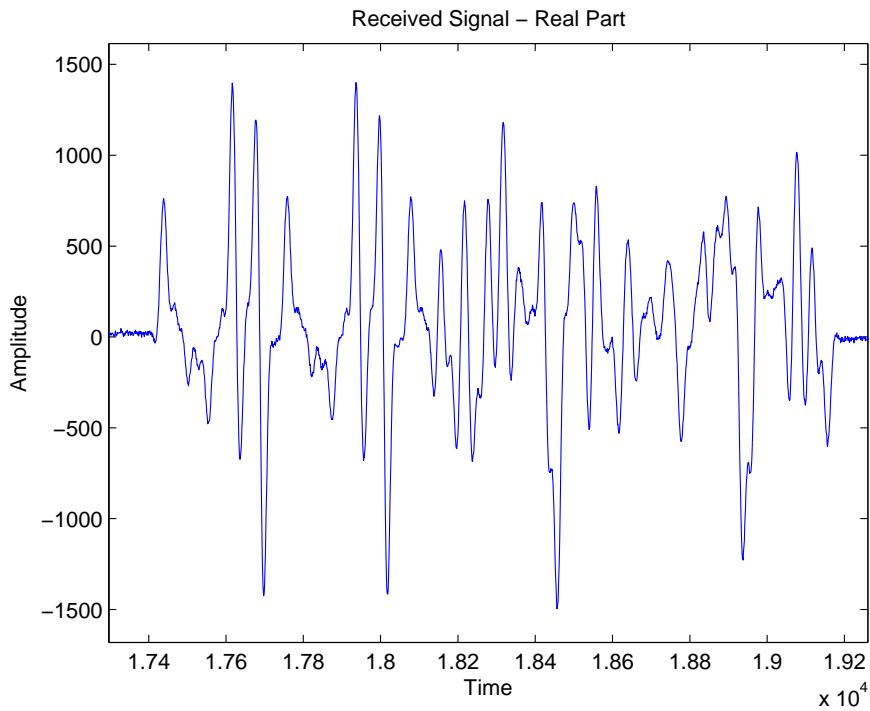


Figure 5.5: Real part of the received signal.

The experiments were conducted in an indoor environment, where the wireless channel between two USRP boards is most likely a flat fading channel. At last, we calculated the bit error rate versus SNR. The performance of the OFDM system is shown in Figure 5.6. The two curves are not exactly the same because in the real environment (using USRPs), it is difficult to measure the exact value of SNR.

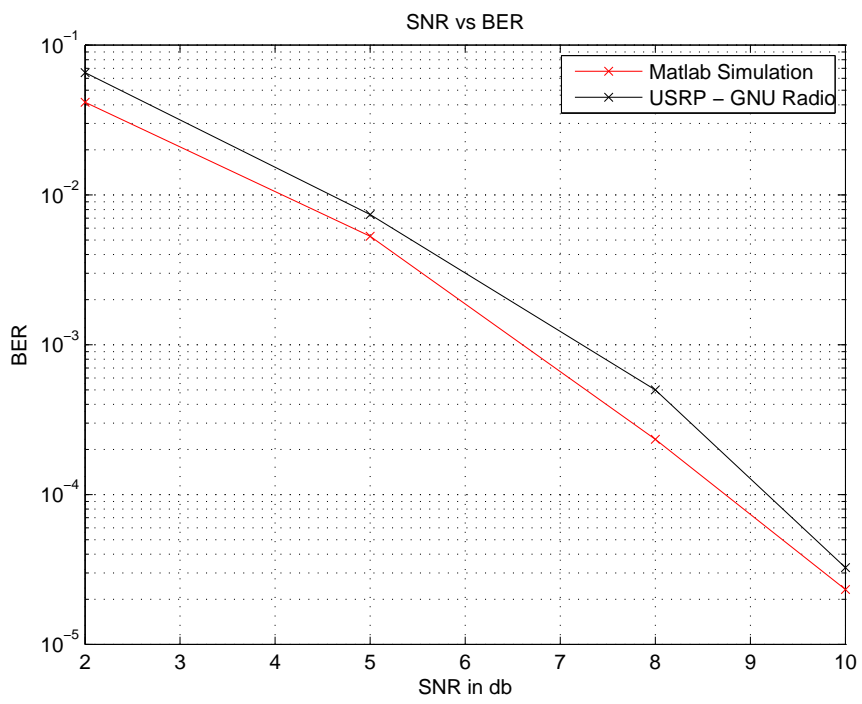


Figure 5.6: Bit Error Rate.

# Bibliography

- [1] Ye Li, Gordon L. Stuber, “*Orthogonal Frequency Division Multiplexing for Wireless Communications*,” Springer, 2006.
- [2] D. Tse, P. Viswanath “*Fundamentals of Wireless Communication*,” Cambridge, 2005.
- [3] Man-On Pun, Michele Morelli, C-C Jay Kuo, “*Multi- Carrier Techniques for Broad-band Wireless Communications*,” Imperial College Press, 2007.
- [4] T. Schmidl and D. Cox, “*Robust frequency and timing synchronization for OFDM*,” IEEE Trans. Commun., pp. 1613-1621, Dec. 1997.
- [5] J. J. van de Beek, M. Sandell, P. O. Borjesson, “*ML estimation of time and frequency offset in OFDM systems*,” IEEE Trans. Signal Processing, vol. 45, pp. 1800-1805, July 1997.
- [6] Hlaing Minn, Vijay K. Bhargava, Khaled Ben Letaief, “*A Robust Timing and Frequency Synchronization for OFDM Systems*,” IEEE Trans. on Wireless Commun., vol. 2, no. 4, July 2003.
- [7] Hlaing Minn, Vijay K. Bhargava, “*On Timing Offset Estimation for OFDM Systems*,” IEEE Comm. Letters, vol. 4, no. 7, July 2000.
- [8] D. Huang, K. B. Letaief, “*Carrier Frequency Offset Estimation for OFDM Systems Using Null Subcarriers*,” IEEE Trans. Commun., vol. 54, no. 5, May 2006.
- [9] Ch. N. Kishore, V. U. Reddy, “*A Frame Synchronization and Frequency Offset Estimation Algorithm for OFDM System and its Analysis*,” EURASIP Journal on Wireless Communications and Networking.
- [10] Xiaodong Cai, Georgios B. Giannakis, “*Error Probability Minimizing Pilots for OFDM With M-PSK Modulation Over Rayleigh-Fading Channels*,” IEEE Trans. on Vehicular Techn., vol. 53, no. 1, January 2004.